Investigation of charge-exciton interactions and their correlations with the device efficiency and operational stability in Phosphorescent Organic Light Emitting Devices by studying delayed electroluminescence

by

Hossein Zamani Siboni

A thesis

presented to the University of Waterloo

in fulfillment of the

thesis requirement for the degree of

Doctor of Philosophy

in

Electrical and Computer Engineering

Waterloo, Ontario, Canada, 2013

AUTHOR'S DECLARATION

I hereby declare that I am the sole author of this thesis. This is a true copy of the thesis, including any required final revisions, as accepted by my examiners.

I understand that my thesis may be made electronically available to the public.

Abstract

Phosphorescent OLEDs (PHOLEDs) have gained a lot of attention due to their remarkable capability of achieving nearly 100% internal quantum efficiency. Although PHOLEDs are a promising technology for the development of high performance display panels and low power consumption lighting sources, their poor operational stability and efficiency decline at high current density (efficiency roll-off) limit their commercialization.

Unlike Fluorescent OLEDs (FOLED) in which singlet excitons are responsible for the device emission, PHOLEDs utilize both singlet and triplet excitons for the emission. However, triplet excitons have much longer lifetime than their counterparts and they can be quenched by two bimolecular interactions (i.e. Triplet-Triplet Annihilation (TTA) and Triplet-Polaron Quenching (TPQ)). These two processes are of particular interests in PHOLEDs, since they directly compete with the radiative relaxation of triplet excitons and therefore, they can considerably reduce the device efficiency. The overall interest of this thesis is to identify and investigate the physical phenomena associated with the efficiency roll-off and electroluminescence degradation in PHOLEDs. This work particularly focuses on understanding the underlying mechanisms associated with TTA and TPQ and their roles in the efficiency roll-off and electroluminescence degradation through the study of delayed electroluminescence.

It is found that efficiency loss due to TPQ is mainly caused by charges within the bulk of the emission layer (EML) rather than by charges at the hole transport layer (HTL)/EML interface. Charges on the guest rather than those on the host are found to be the most efficient in quenching excitons, revealing that guest polaronic species are the most detrimental to device efficiency. In addition, recombination of electrons and holes on the host material generally leads to higher device efficiency in comparison to the case where recombination happens on the guest material. Although electron-hole recombination on the host tends to produce higher device efficiency, host e-h recombination is generally also associated with significant efficiency roll-off due to the quenching of the host triplet excitons primarily as a result of host-host TTA.

Furthermore, results from the study of devices with various guest concentrations reveals that as the concentration of the guest molecules increases and the creation of host triplet excitons subsides (since most e-h recombination occurs on the guest) host-host TTA decreases, hence also the efficiency roll-off. In such case, quenching is mostly caused by polarons residing on guest sites. At optimum guest concentrations (~8 % Vol.), a balance between host e-h recombination and guest e-h recombination is reached, and thus also minimal TTA and TPQ.

Based on the findings from the investigation of efficiency roll-off during short-term device operation, we extended our study to understand the mechanisms associated with the gradual efficiency loss in the devices during long-term operation. Two distinctive degradation mechanisms are observed in PHOLEDs, depending on whether the device contains a hole blocking layer (HBL) or not. For a device without a HBL, excess holes penetrate into the electron transport layer (ETL), and lead to the deterioration of the ETL adjacent to the interface of the emitting layer. The lower electron transport capacity of the degraded ETL alters the balance in hole/electron injection into the emitting layer, and results in a decrease in the

luminescence efficiency of the PHOLEDs. For a device with a HBL, on the other hand, holes accumulate and become trapped in the emitting layer, and result in a decrease in the luminescence efficiency of the PHOLEDs, due to their role in acting as exciton quenchers or as non-radiative charge recombination centers. Furthermore, the results show a strong correlation between the extent of hole blockage capacity of the HBL and the deterioration in device EL efficiency, pointing to the major role that the build-up of hole space charges in the emitting layer plays in EL degradation. In this case, gradual increase of trapped charges in the EML enhances the TPQ process and hence exciton quenching manifesting as a reduction of TTA. In addition, gradual increase in driving voltage often observed with prolonged electrical driving of PHOLEDs is mainly governed by the accumulation of holes at this interface. Reducing the build-up of hole space charges in this region, for example, by means of eliminating guest molecules from the vicinity of the interface, leads to a significant improvement in the stability of PHOLED driving voltage.

Acknowledgments

I would like to express my sincere gratitude to my supervisor Professor Hany Aziz for his guidance and continual support during my research. His invaluable knowledge, inspiration and insights guided me all the way throughout this challenging journey.

I would like to acknowledge my advisory committee, Professor Siva Sivaththaman, Professor Yuning Li and Professor Dyan Ban for reviewing my work and their valuable comments and suggestions. I would like to thank Professor Suning Wang who accepted to be my PhD external examiner.

I would like to thank Mr. Richard Barber (Giga to Nano (G2N) Lab manager) and Mr. Robert Mullins for their invaluable technical assistance.

My special thanks to my colleagues, Dr. Yichun Luo, Mr. Qi wang, Mr. Graeme Williams, Mr. Michael Zhang, Miss. Uyxing Vongsaysy, Mr. Thomas Borel, Mr. Sibi Sutty, Mr. Yoshitaka Kajiyama, Mr. Baolin Tian and Miss. Radhika Phatak.

I want to express my appreciation to all my friends who supported me during my PhD study, including but not limited to Dr. Azad Qazi Zade, Dr. Hamid Reza Molavin, Mr. Roozbeh Rashedi, and Mr. Babak Doulatyari.

I would like to thank my parents and my sister for their continual love and support.

Finally, I thank the National Research Council of Canada for the financial support during my research.

Contents

List of Tables:

List of Figures:

List of Abbreviations

OLED	Organic Light Emitting Device
PHOLED	Phosphorescent Organic Light Emitting Device
HOMO	Highest Occupied Molecular Orbital
LUMO	Lowest Unoccupied Molecular Orbital
ITO	Indium Tin Oxide
HTL	Hole Transport Layer
ETL	Electron Transport Layer
HBL	Hole Blocking Layer
EML	Emissive Layer
EL	Electroluminescence
PL	Photoluminescence
IVL	Current-Voltage-Luminance
TTA	Triplet-Triplet Annihilation
TPQ	Triplet-Polaron Quenching

Chapter One: Introduction and background

1.1 History of OLED

Electroluminescence (EL) is a phenomenon which converts electrically generated excited states into light. EL of organic materials was first observed in 1953 by Bernanose et al. [1]. Following this observation, several works were published which studied the EL of single crystal anthracene [2-4]. However, at that time devices had very poor efficiency and required a significantly high driving voltage to emit. The first practical thin film OLED based on small molecule organic material with high efficiency was reported by Tang et al. in 1987 [5]. Their device structure consisted of two separate layers that served as hole transport and electron transport mediums, which significantly reduced the driving voltage and enhanced the light output. Following Tang's work, in 1990 Burroughes et al. [6] developed a highly efficient green polymer based OLED by incorporating a single layer of Poly(p-phenylene vinylene) (PPV) .

In the late 1990s, another breakthrough work was reported by Baldo et al. which demonstrated a highly efficient OLED based on phosphorescent emitter [7]. According to the spin statistic theory, electrical excitation of the organic material generates 25% singlet excited states and 75% triplet excited states. In Fluorescent OLED, due to the forbidden transition from the excited triplet state to the ground state, only singlet excitons contributed to the light emission. However, in phosphorescent materials because of the heavy metal atom complexes in their molecular structure, due to the spin orbit coupling effect, triplet excitons also contribute to the light emission leading to the maximum theoretical efficiency of 100% [8].

1.2 Phosphorescent OLED (PHOLED)

A typical PHOLED structure consists of a hole transport layer (HTL), an electron transport layer (ETL), and an emission layer (EML). Transparent Indium-Tin-Oxide (ITO) is usually used for the anode and alloy of magnesium: silver (Mg:Ag) or Lithium Fluorid/Aluminum (LIF/AL) is employed for the cathode. All of the organic materials are vacuum deposited on the transparent substrate. Upon applying a forward bias to the electrodes, electrons and holes are injected into the ETL and HTL, respectively. The injected holes and electrons are transported by a hopping mechanism on the Highest Occupied Molecular Orbital (HOMO) of HTL and Lowest Unoccupied Molecular Orbital (LUMO) of ETL, respectively. Opposite charge carriers then meet each other in the EML and form electron-hole pairs called excitons. EML is based on a mixture of host-guest molecules in which phosphorescent emitter molecules are doped into the host matrix. The host acts as a transport medium for charge carriers and prevents the aggregation of guest molecules [9]. Upon electrical excitation, excitons can be formed on both host and guest molecules. Proper concentration of guest molecules and energy alignment between the host and guest can effectively suppress the emission from the host molecules [10]. However, in the state of the art PHOLEDs, devices have more complex structures and employ additional layers (e.g. charge injection layers and charge blocking layers) to achieve high efficiency [11-16].

1.3 General

A display is a device that presents information in a visual form such as text, images, and videos. A display device can be used as an interface between human and machine or else as an output device. With the growth of technology and demands, the next generation display panels

require display devices that have low power consumption, high contrast ratio, wide viewing angle, high image quality, and long operational lifetime.

One of the first technological advancements in the display field is the invention of Cathode Ray Tube (CRT) in the 19^{th} century. However, due to their heavy weight and bulky characteristics, application of CRT displays in today's electronic devices is rare.

Another major technological advancement in the display field is the emergence of flat panel displays such as Plasma Display Panels (PDPs) and Liquid Crystal Display (LCD) panels. In comparison to the traditional CRT displays, flat panel displays offer a larger screen size, higher resolution, lower weight, thinner width, and higher image quality. However, flat panel displays have several drawbacks that limit their application. For example, PDPs have a relatively large pixel pitch, which makes them only suitable for very large display panels. High power consumption, image burn-in, and low lifetime are other important issues associated with PDPs. LCDs are possibly the leading technology in today's display devices in both industrial scale and home entertainment and consumer electronic products. In LCDs, each pixel has two transparent electrodes along with two polarizer films in which liquid crystal material is sandwiched. Depending on the applied voltage to the pixel, liquid crystal molecules change their shape in a way that blocks or passes the light. However, LCD does not emit light and therefore requires a lighting source. In traditional LCD, fluorescent light source was used as a backlight. In modern LCDs, fluorescent backlight has been replaced with efficient light emitting diodes (LEDs) in order to reduce power consumption. Although there have been numerous improvements on LCD performance, they suffer from narrow viewing angle, poor response time, low contrast ratio, and poor colour accuracy, which limit LCD's future use in the next generation of display panels.

Over the past decade a significant amount of research has been focused on the development of Organic Light Emitting Devices (OLEDs) as a new technology for the next generation of display panels [5,17-24]. The main advantage of OLEDs in comparison to LCD is their self-luminous characteristic that does not require any backlight for operation. Self-luminosity makes these display panels extremely thin and portable; this considerably reduces power consumption. Panels made with OLEDs have a wide view angle and high brightness that make them suitable for both indoor and outdoor use. Besides, molecules in organic semiconductor are bonded with Van der Waals forces; therefore, OLEDs are flexible and can be easily fabricated on plastic substrates.

Particular attention has been focused on Phosphorescent OLEDs (PHOLEDs) due to their capability of achieving nearly 100% internal quantum efficiency [25][21]. Unlike Fluorescent OLEDs (FOLED) in which singlet excitons are responsible for the device emission, PHOLEDs utilize both singlet and triplet excitons; therefore, they have much higher efficiency than FOLED. This high efficiency and easy colour tunability make PHOLEDs a better choice in comparison to FOLEDs for future display panels.

When it comes to other applications, OLEDs are possibly the strongest candidate for solid state lighting [26]. Nearly 20% of the world's electricity is consumed by lighting. Overall, this amount of electricity is responsible for the production of 1,900 million tons of greenhouse gas emissions [27]. For the past several years, incandescent light bulbs have been considered a main source of lighting. These light bulbs can produce light with colour temperature close to sunlight with excellent Colour Rendering Index (CRI). However, their efficiency is only about 10 to 20 lm/W and the majority of input electricity is converted into heat. For more efficient lighting, Compact Fluorescent Lamp (CFL) is an alternative light source that has the efficiency of about 40 to 60 lm/W. However, over the past decades several countries have replaced the incandescent

light bulb with CFL. Nevertheless, high user cost and requirements for specific disposal procedures after operational lifetime make CFL not an appropriate lighting source for the future. OLEDs with colour tunability can produce light that covers a wide range of visible spectrum and therefore light with very high CRI. In addition, low power consumption and flexibility make OLED a promising technology for future lighting applications.

Intense research has been focused on the improvement of the efficiency of the OLED, resulting a successful fabrication of white PHOLED with an efficiency of more than 100 lm/W [28]. Generally in OLEDs, high efficiency can be achieved at high current range. However, OLEDs show efficiency roll-off at this current range [29], which is more noticeable in PHOLEDs because of their long lifetime emitter species. Although several approaches have been proposed to reduce efficiency roll-off [13,16,16,30,31], the physical phenomena associated with this are still not fully understood.

Generally upon electrical excitation and formation of excitons, bimolecular interactions (i.e. Triplet-Triplet Annihilation (TTA) and Triplet Polaron Quenching (TPQ) take place in the emission layer. These processes arise from a long lifetime of triplet excitons, which typically range between microsecond and millisecond. These two processes are of particular interest in PHOLEDs, since emitter species are triplet excitons and can be quenched by these interactions. Numerous reports have pointed out that these bimolecular interactions are the main sources of efficiency roll-off in PHOLEDs. However, only a few studies have been devoted to understand the mechanisms associated with TTA and TPQ in PHOLEDs [29,32-34]; therefore, more fundamental studies related to these processes are still required. For example, it is still not clear whether TPQ is mainly associated with the presence of charge carriers on the guest molecules or on the host and it is not known how this process affects the emission mechanism and efficiency

of the PHOLED. In addition, it is believed that TTA mainly occurs between the guest excitons [29], while the role of host-host TTA to the device efficiency and efficiency roll-off remains unknown.

Although OLEDs demonstrate superior performance among other display devices, their commercialization has so far been limited, in part due to the limited operational stability. Display panels based on OLEDs have a lifetime far shorter than other display devices [35]. Several factors affect the OLED's operational stability and in general they can be categorized as an extrinsic degradation and intrinsic degradation [36-38]. However, proper encapsulation can effectively eliminate the extrinsic degradation [36-39]. Intrinsic degradation - the most important source of degradation - refers to a luminescence loss upon removal of extrinsic degradation. Intrinsic degradation can be due to the chemical instability of the materials [20,40] used in the device and/or physical phenomena [23,41] within the device that accelerate the luminescence loss. Several studies have addressed the issues related to the OLEDs' operational stability with most studies based on conventional fluorescent OLEDs (FOLEDs). Only a few studies related to the operational stability of PHOLEDs are available; thus, the development of PHOLEDs with long operational stability is still a challenging issue. Because of the different emitter species in FOLED and PHOLED, the reasons behind the degradation of fluorescent OLEDs are not necessarily applicable to PHOEDs; therefore, more studies are required in order to provide general models that describe the physical mechanisms behind their poor stability.

1.4 Motivation

In general, PHOLEDs emission is a result of two mechanisms: i) e-h recombination on the guest molecules and ii) e-h recombination on the host followed by energy transfer to the guest. The former mechanism mainly arises from the charge trapping characteristics of the guest emitter in the host matrix. On the other hand, the second mechanism is the principal mechanism when charge trapping effect by the guest dopant is insignificant. Although a lot of work has been focused on the investigation of efficiency behaviours in PHOLEDs, it is still an open question of which mechanism leads to higher efficiency.

Generally, efficiency of the PHOLEDs reduces significantly at high guest concentration. In this regard, high efficiency can be achieved at optimum guest concentration. The general models describing the low efficiency of the devices with high guest concentrations are i) the TPQ by the presence of trapped charges on the guest and ii) quenching of triplet excitons by guest-guest TTA process. However, high efficiency roll-off in case of devices with low guest concentration cannot be fully explained by these mechanisms and therefore requires further investigation to understand this efficiency roll-off behaviour.

Efficiency of PHOLEDs can be affected significantly by the TPQ process. Due to the HOMO energy level differences between the HTL and EML, holes can accumulate at the interface of HTL/EML. Therefore, efficiency can decrease significantly by the TPQ primarily due to the charges that accumulate at the HTL/EML interface as a result of the interfacial hole injection barrier. However, other results suggest that the TPQ is caused mostly by charges within the EML bulk. As such, the nature of the underlying polaronic species and their location within the device

remain unclear, making it difficult to devise approaches to reduce them and improve device efficiency.

Along with efficiency roll-off, another technical issue of PHOLEDs is the insufficient operational stability which limits the wide commercialization of this technology. In order to enhance the device efficiency, charge carriers and excitons must be confined within the EML. For this purpose, it is customary to include hole blocking layers (HBLs) to confine holes (and excitons) within the EML and prevent them from reaching the ETL. However, devices with a HBL usually have a lower stability than their counterparts without a HBL. Therefore, it is not clear whether the lower stability is associated with the presence of hole space charge and subsequent TPQ or not. Moreover, the extent to which hole space charges can accelerate the device stability is not known.

Contrary to electroluminescence stability, the root causes behind the increase in OLED driving voltage during prolonged electrical driving have not been carefully investigated, and remain essentially unknown, especially for PHOLEDs. The driving voltage stability is, on the other hand, an important issue, especially for active matrix display panels in which each pixel is driven by its own integrated circuit. Since the circuits are typically designed to provide a certain power output, a significant change in the voltage required to drive an OLED creates challenges for driving circuits. Therefore, the last part of this thesis is allocated to investigating and studying the causes of voltage rise during device operation.

1.5 Objectives

This work aims to study delayed electroluminescence (EL) for the purpose of identifying and investigating the physical phenomena behind the efficiency roll-off and electroluminescence degradation in PHOLEDs. This study particularly focuses on understanding the underlying mechanisms associated with TTA and TPQ and their roles in the efficiency roll-off and electroluminescence degradation through the study of delayed EL. To date, no comprehensive investigation is available that explores mechanisms underlying bimolecular interactions in PHOLEDs and offers a better understanding of their correlations with the efficiency roll-off and operational stability through the study of delayed EL. In addition, since delayed EL emission arises only from the EML, even in devices with complex structures that contain several layers it is possible to selectively study the EML without restriction.

Detailed objectives of this thesis are as follows:

- Identify the roles of host versus guest e-h recombinations in the efficiency behavior of PHOLEDs.
- Identify the role of host excitons in the TTA and TPQ processes and their subsequent effects on the efficiency roll-off.
- Investigate whether exciton quenching by the TPQ process at the charge transport layer/emission layer interface is due to interfacial charges or charges in the bulk.
- Investigate the possible correlation between the presence of bimolecular interactions and electroluminescent stability.

- Understand to what extent bimolecular interactions, particularly TPQ, accelerates EL degradation, and in this case, identify how charge accumulation within the EML affects the device EL stability.

- Uncover the causes of driving voltage rise in PHOLEDs and investigate whether or not voltage rise correlates with EL degradation.

1.6 Thesis organization

Chapter one is a general introduction of this thesis and covers the motivations and objectives of this work.

Chapter two is a brief review of the physics of OLEDs. This chapter covers a variety of subjects related to the organic semiconductor and OLEDs such as excitons and polarons in organic semiconductors and bimolecular interactions associated with them. At the end of this chapter a brief review of delayed electroluminescence and sources of this emission in PHOLEDs are provided.

Chapter three is related to the experimental and device fabrication procedures.

Chapters four and five are dedicated to the studies related to the efficiency and efficiency roll-off in PHOLEDs. These chapters cover the underlying mechanisms associated with TTA and TPQ during short-term device operation. . Chapter four focuses on the emission mechanisms in PHOLEDs with the aim of understanding which one leads to higher efficiency. Then, the role of each bimolecular interaction on the efficiency roll-off is discussed. Chapter five first discusses whether TPQ is associated with the presence of charges on the guest or on the host. Next, bulk

and interfacial TPQ processes are investigated in order to understand which one more dominantly reduces the efficiency.

Chapters six, seven, and eight introduce studies related to the operational stability in PHOLEDs. The findings from the previous chapters will be used to study the bimolecular interactions during long-term device operations. Chapter six investigates whether or not TPQ accelerates the electroluminescence degradation. Chapter seven determines to what extent bimolecular interactions reduces PHOLEDs lifetime. Chapter eight covers a different aspect of PHOLEDs operational stability, and investigates the causes of driving voltage rise in PHOLEDs during device operation by studying bimolecular interactions before and after electrical aging. This chapter concludes by providing a method to reduce the voltage rise.

Chapter nine summarizes the results and provides suggestions for future works for the development of highly efficient and stable PHOLEDs.

Chapter Two: Literature review

2.1 Excitons and polarons in organic semiconductor

In organic semiconductors, the presence of charge carrier in a molecule causes a lattice distortion. Charge carrier and its surrounding lattice distortion is called polaron. This lattice distortion typically changes the energy state of the molecules, which means that HOMO and LUMO energy levels shift respectively upward and downward to reduce the total energy of the molecule [42]. Since organic materials have disordered molecular structures and molecules are bonded with weak van der Waals forces, mobility in organic semiconductors is much lower than inorganic semiconductors, which is in the range of 10^{-7}-10^{-3} cm^2/VS for holes and is a few orders of magnitude lower for electrons [43]. This is mainly a result of weak interactions between the molecular orbitals of lattice sites that form a narrow band. Therefore, charge transport in the organic semiconductor is the motion of polarons and charge carriers via hopping between the localized states [42,44-46].

An exciton is an energy state of an electron-hole pair. Excitons in the organic semiconductor can be formed either by absorption of photon or by injection of the charge carriers into the semiconductor. Due to the strong columbic interaction between the electron-hole pair, excitons in organic semiconductors are Frenkel and are localized in a single molecule. When considering spin of an electron in energy state, excitons can be categorized as singlet or triplet. In singlet exciton, spin of an electron in the excited state is paired with the ground state. In triplet excitons, spin of an electron is parallel with the ground state. Photo excitation in organic semiconductor can only create singlet excitons while electrical excitation can produce both singlet and triplet

excitons. Upon electrical excitation, following the spin statistic theory, 25% of the created excitons are singlets and 75% are triplets.

Electrons in an excited state can follow different types of electronic transitions. Figure 2.2 shows a Jablonski diagram of the electronic energy states in the organic molecule. Internal Conversion (IC) is a radiationless transition from the higher excited state to the lower excited state of the same multiplicity. Another radiationless electronic transition is an Intersystem Crossing (ISC). This transition occurs between the singlet and triplet states and requires a spin change of an electron. This transition is more pronounced in phosphorescent materials because of the strong spin-orbit coupling effect. There are two types of radiative transitions in organic molecules: fluorescent transition is the electronic transition from the excited singlet state to the ground state and phosphorescence transition is the electronic transition from the excited triplet state to the ground state. Normally ground state in organic molecule is a singlet state; therefore, the fluorescent transition is allowed. Unlike the fluorescent emission, the phosphorescent emission is a forbidden transition and requires a spin flip of an electron. This process is facilitated in the materials that contain heavy metal atoms in their molecular structure where a strong spin-orbit coupling effect exists [7].

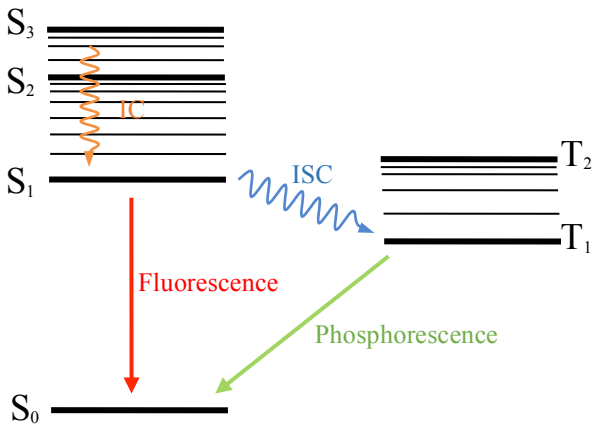

Figure 2.1 Electronic energy states in organic molecules

2.2 Energy transfer

Two common types of energy transfers between the molecules in organic semiconductor are Forster and Dexter energy transfers. Figure 2.3 illustrates the mechanisms of these two energy transfer processes. In the Forster energy transfer, donor excited state (D^*) transfers its energy to the acceptor (A) molecule via a dipole-dipole interaction within a range of up to 10 nm. Forster energy transfer requires the spectra overlap of the emission of the donor and absorption of the acceptor. In this electronic transition, spin of an electron is conserved in both donor and acceptor molecules and therefore it is a very efficient energy transfer for singlet excited states. Since this energy transfer does not require a spin-flip of the electron, this process is more dominant in fluorescent material.

Dexter energy transfer involves the exchange of electrons between the donor and acceptor molecules. This transfer process requires a molecular orbital overlap of the donor and acceptor molecules and therefore it is a short range process below 1 nm. Since this energy transfer involves the physical exchange of the electrons, triplet excitons can be effectively transferred by

this process. Dexter energy transfer is the effective energy transfer mechanism in phosphorescent materials.

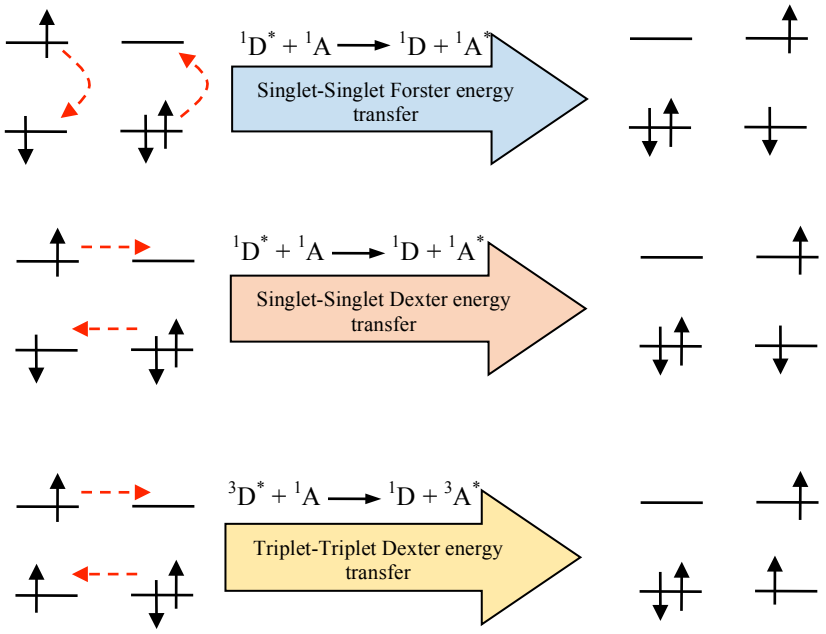

Figure 2.2 Forster and Dexter energy transfer mechanisms

2.3 Bimolecular interactions

2.3.1 Triplet-Triplet Annihilation (TTA)

Triplet-Triplet Annihilation (TTA) is a process that involves the fusion of two triplet excitons. TTA can lead to the formation of singlet state and subsequent delayed fluorescent emission (because typically the energy of two triplet excitons is higher than the singlet excited state) [47], or TTA can form a triplet exciton. TTA process has the following reactions:

$$T^* + T^* \rightarrow S^* + S_0 \quad (1)$$

$$T^* + T^* \rightarrow T^* + S_0 \quad (2)$$

In a crystalline material, TTA was first observed on the delayed fluorescence from the single crystal anthracene [48]. Since then, particular attention has been given to this process in fluorescent materials [49-51]. It is assumed that the 25% singlet excited state production results in the maximum theoretical quantum efficiency of 25%. However, several works have been reported which surpass the maximum theoretical limit of the efficiency in FOLED. For example, it has been shown that TTA can have a significant contribution to the device emission [52-54]. Considering the contribution of the generated singlet excitons produced by the TTA process to the device emission, FOLEDs can have more than 40% internal quantum efficiency [53].

In contrast to FOLED, TTA can effectively reduce the efficiency in PHOLEDs. Baldo et al. [29] studied the transient analysis of TTA in various host:guest systems. In their experiments they demonstrated that in a host:guest system where triplets are confined on the guest molecules, guest-guest TTA can significantly reduce the device efficiency. On the other hand, in a system where both endothermic and exothermic energy transfers between the host and guest occur, efficiency roll-off cannot be simply explained by the guest-guest TTA. In such a system, it was

suggested that host-guest TTA can also contribute to the efficiency roll-off, although no direct evidence for this process has been shown. Next, Reineke et al. [34] proved that in a system with a small difference on the triplet energy levels of host and guest, host-guest TTA at high current density plays a limiting factor in suppressing the efficiency.

2.3.2 Triplet-Polaron Quenching (TPQ)

Interaction of triplet excitons with polarons is called triplet-polaron quenching. This interaction results in an energy transfer between the triplet exciton and polaron and subsequent formation of polaron with higher energy state and a singlet ground state [55]. Charge imbalances in the EML [56-58], presence of charge traps in the material [59], different hole and electron mobility values of the charge transport layers, and EML and charge accumulation at the interfaces [60] of the layers can significantly aggravate this quenching process. Time evolution of triplet density, assuming the presence of both TTA and TPQ in the EML, can be described by the following equation [61]:

$$\frac{d[T]}{dt} = -\frac{[T]}{\tau} - \gamma_{TT}[T]^2 - \gamma_{TP}[T] \qquad (3)$$

Where [T] denotes the concentration of triplet exciton, τ is the lifetime of triplet excitons, and γ_{TT} and γ_{TP} are the bimolecular annihilation rate constants for TTA and TPQ, respectively. According to the above equation, TTA has a quadratic relation to the triplet excited state density while TPQ depends linearly on the concentration of triplet excitons. It has been shown that both annihilation processes can contribute to the efficiency roll-off [32]. However, the influence of TTA on the efficiency roll-off is small at low current density and TPQ is found to be the source

of efficiency roll-off at this range. On the other hand, TTA becomes the dominant annihilation process at high current density due to its quadratic relation with triplet exciton density. In addition, thickness of the emission layer and width of the recombination zone are found to be the critical factors enhancing the bimolecular interactions. Narrow recombination zone can effectively increase the population of triplet excitons; hence TTA, and thinner film can increase the concentration of charge carriers and consequently TPQ [50]. To that end, charge balance in the system can widen the recombination zone and reduce the annihilation processes [62,63].

2.4 Reliability and degradation

Degradation of OLEDs can be categorized into two major groups: extrinsic degradation and intrinsic or long-term degradation,

2.4.1 Extrinsic degradation

Extrinsic degradation is mainly associated with degradation phenomena at the electrode contacts which create non-emissive dark spots [36-38]. Formation of the dark spots arises from the growth of non-emissive defects during device operation that eventually cover all of the emissive area. It has been shown that delamination at the organic/metal interface is the primary reason behind the formation of the dark spot. Ambient moisture penetration through the metal and the decomposition of organic layer due to the Joule heating effect are both responsible for the cathode delamination; this causes poor adhesion between the cathode and the organic layer. However, encapsulation of the entire device or keeping the device in the nitrogen ambient can effectively suppress this degradation mechanism.

2.4.2 Intrinsic degradation

Intrinsic degradation is the reduction of luminance intensity in the absence of ambient effect [19,64]. Several mechanisms have been proposed to address the chemical and physical phenomena associated with intrinsic degradation. It has been shown that certain materials are unstable due to the presence of certain charged species [20]. Tris(8-hydroxyquinoline)aluminum (Alq_3), a widely used fluorescent material, is unstable due to the presence of positive charges. Unstable cationic Alq_3 molecules act as an exciton quencher and nonradiative recombination centers, which reduces the luminance intensity. It has been shown that doping HTL with dopants that act as hole traps, significantly improves the device lifetime [65]. Following the Aziz work, Luo et al. demonstrated that upon the formation of electron space charge in Alq_3, electrons can also induce photoluminescence degradation of Alq_3 [66].

Kondakov et al. reported that build-up of positive space charges at the interface of HTL/ETL in bi-layer OLED is responsible for luminescent decrease [67]. Analyzing the driving voltage profile during the long-term device operation revealed that long-term luminescent decrease correlates linearly with the build-up of positive space charges at the interface of HTL/ETL.

Lee et al. proposed another model for long-term degradation in OLEDs [68]. According to this model, diffusion of indium ions from the ITO surface into the adjacent organic layer during long-term device operation is responsible for electroluminescent degradation.

Giebink et al. identified exciton-polaron annihilation as a principal defect formation route in PHOLEDs [23,41]. It was proposed that energy transfer from an exciton to a polaron leaves a charged molecule that is prone to the bond cleavage. Scholz et al. proposed that a chemical

reaction between the emitter and adjacent charge transport molecules is also responsible for EL degradation [40]. Sivasubramaniam et al. [69] suggested that degradation of HTL can also reduce the operational stability of the device. In this case new products as a result of dimerization or bond cleavage of HTL have lower singlet or triplet energy states, which can quench the emitter excitons and further reduce the device operational lifetime.

2.5 Efficiency roll-off

Efficiency roll-off is another important aspect of OLEDs, which is associated with efficiency loss at high current density. This is more pronounced in PHOLEDs because of the long-lived triplet emitter excitons [29]. Baldo et al. reported that efficiency roll-off is mainly attributed to the TTA. In this regard phosphorescent molecules with short triplet exciton lifetime can effectively reduce the efficiency roll-off. Giebink et al. [70] reported that loss of charge balance at low current density is responsible for efficiency roll-off. Furthermore, Reineke et al. [32] suggested that along with TTA, TPQ is also responsible for the device efficiency roll-off.

In addition to fundamental studies related to the efficiency roll-off mechanisms, several studies have focused on improving the efficiency of PHOLEDs through the device engineering. Meerheim et al. systematically studied the effects of HBLs on the device efficiency. They showed that improving charge balance in the EML and energy level alignments between the EML and charge transport layers can significantly enhance the device efficiency [71,72]. Goushi et al. studied devices with various HTLs in order to investigate their roles on the confinement of triplet excitons on $Ir(ppy)_3$ emitter. They showed that back energy transfer from the emitter into the adjacent HTL can significantly reduce the device efficiency. In this regard, HTL with higher

triplet energy level than emitter can effectively confine triplet excitons on the emitter and improve the efficiency of PHOLED. Pfeiffer et al. showed that reducing the voltage drop across the organic layer by doping the charge transport layers with donor and acceptor dopants can noticeably enhance the efficiency of the PHOLEDs [73,74]. Along with the works related the modification and optimization of the charge transport layers, several works have been dedicated to the modification of emission layer in order to improve the device efficiency. D'Andrade et al. demonstrated that fluorescent efficiency of fluorescent emitter can be enhanced significantly by doping the EML with phosphorescent sensitizer. In this case efficient energy transfer of both singlet and triplet excitons from $Ir(ppy)_3$ into the fluorescent dopant was suggested to be the mechanism of efficiency improvement. They also showed that devices with double doped EML show less efficiency roll-off in comparison to the PHOLEDS based on $Ir(ppy)_3$ due to reduced TTA as a result of fast energy transfer from $Ir(ppy)_3$ into florescent emitter [75]. Chin et al. [76] showed that controlling the doping profile of emitter in the EML can also enhance the efficiency. Increasing guest concentration at the HTL/EML interface where recombination zone is located improves the exciton confinement on the guest and therefore enhances the efficiency.

2.6 Delayed EL

Delayed EL is a persistent electroluminescence emission after a removal of external bias. Delayed EL was first observed in anthracene crystal by Kepler in 1963 [48]. In organic semiconductors, electron-hole recombination creates singlet and triplet excitons. In fluorescent materials, the typical lifetime of singlet excited states is on a scale of *ns* while the lifetime of triplet excitons is in a *ms* or μs range. Therefore, EL from the fluorescent materials can have two components. The first component is associated with the fast relaxation of the singlet excited state

and the second slow component (delayed EL) originates from the TTA of the long-lived triplet excitons [47] and recombination of de-trapped charges. Recently, several published reports have covered the aspects of this slow process to the efficiency of the FOLED [52-54]. Interestingly, it has been shown that delayed EL can significantly affect the device performance and efficiency. Contribution of the singlet states produced by the TTA process can effectively increase the maximum 25% theoretical limit of efficiency to nearly 60%. Kondakov also reported that delayed EL can contribute up to 50% of the steady state EL emission [53].

In PHOLEDs, delayed EL emission is associated with the following processes: (i) recombination of trapped charges that get released after the end of the forward bias pulse; (ii) slow migration of host triplet excitons that are generated during the electrical excitation and their late arrival to the proximity of guest sites where energy transfer to the guest can take place; and (iii) TTA. Process (i) is more pronounced in PHOLEDs because of EML's host:guest structure in which guest molecules typically trap charge carriers and the subsequent recombination of trapped charges produces delayed EL.

Chapter Three: Experimental

The following chapter presents the device fabrication and measurement procedures that are used in this work. At the end of the chapter, a detailed description of the measurement setup of delayed EL is given.

3.1 Device fabrication

3.1.1 Substrate preparation

In this work, commercially available patterned Indium-Tin-Oxide (ITO) films on the glass substrates from Luminescence Technology Co. are used. Figure 3.1 shows a schematic of the patterns ITO. ITO substrates are cleaned with micro-90 optical cleaner for 10 minutes in an ultrasonic bath. Next, substrates are cleaned with acetone and isopropanol alcohols for 15 minutes, respectively. Afterwards, substrates are dried with nitrogen gun and then heated at 100^{o} C for approximately 10 minutes in order to remove any remaining moisture from the surface. Prior to the material deposition, substrates are treated with CF_4/O_2 plasma in a Reactive Ion Etching (RIE) chamber.

3.1.2 Material deposition

Angstrom Engineering EVOVAC evaporation system is used for material deposition. Organic materials and cathode metals are deposited using thermal evaporation technique in a vacuum at a base pressure of 5×10^{-6} torr. Organic materials are deposited at the rates between 0.2-2 A^{o}/s. Depositions rate is controlled automatically at the target rate by a controller.

In co-evaporation mode, deposition rate of each material is monitored with a separate crystal sensor for precise evaporation. In this work, PHOLEDs based on archetypical 4,4'-bis(carbazol-9-yl)biphenyl (CBP) and Tris(2-phenylpyridine)iridium(III) [$Ir(ppy)_3$] host:guest phosphorescent system in the emitting layer are used. In these devices, N,N'-di(naphthalene- 1-yl)-N,N'-diphenyl-benzidine (NPB) or CBP is used to form the HTL. Aluminum tris(8)- hydroxyquinoline (Alq_3) and 1,3,5-tris(N-phenylbenzimidazol-2- yl)benzene (TPBi) are utilized for the ETL. In some cases, a 2,9-dimethyl-4,7-diphenyl-1,10-phenanthroline (BCP) and aluminum (III) bis(2-methyl-8-quinolinate)-4-phenylphenolate (BAlq) HBLs are inserted between the emitting and electron transport layers.

3.2 Device test and characterization

Device performance measurements and characterizations are carried out immediately following the device fabrication. During the test, the devices are kept in a nitrogen ambient to prevent the ambient induced degradation. Luminance of the devices is measured with CS-100A Minolta chromameter. Current (I)-Voltage (V)-Luminance (L) measurements are completed with Agilent 4155C semiconductor parameter analyzer.

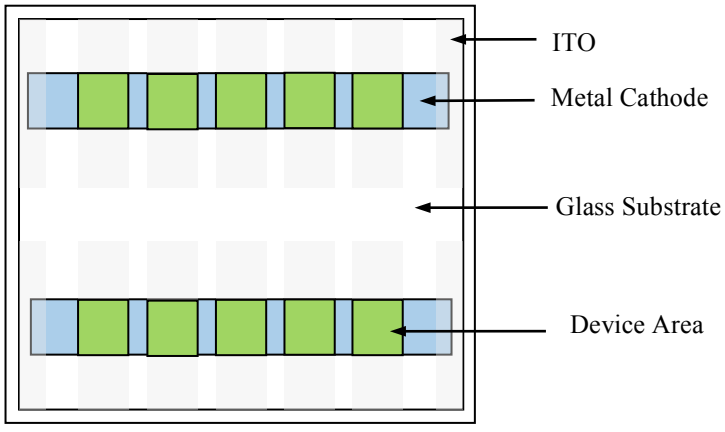

Figure 3.1 Schematic structure of patterned ITO and device active area

3.3 EL stability measurements

EL stability of the devices is tested by using an Alternative Current (AC) with a 50% duty cycle and a frequency of 60 Hz to prevent any metal ion diffusion from the electrodes through the organic layers and excessive charge accumulation at the interfaces of organic layers. EL intensity is collected by using silicon photodiode along with continuous recording of the device's forward voltage. Devices are aged to 50% of initial brightness with the current density of 20 mA/cm^2.

3.4 Delayed EL measurements

Delayed EL intensity of the devices is collected by a fiber optic connected to the photodetector. An optical chopper is placed between the device and the fiber optic in order to block the prompt EL light during the application of forward bias. An R928 photomultiplier tube equipped with a 700-nm short-wavelength pass filter is used to record the time-resolved delayed EL emission. The photomultiplier current is amplified by an Ithaco Model 1211. Tektronix digital oscilloscope is used to record the delayed EL data. Stanford Research System model DG535 digital delay generator is used to implement the timing setup. Figure 3.2 shows the timing setup of the delayed EL measurement system. Home built amplifier is used to apply various magnitudes of forward and reverse voltage pulses. A forward bias pulse of 10V with a pulse width of 0.5 ms, which is long enough to promote excitons to the steady excited states, is applied to the devices. During the forward bias pulse, the optical chopper prevents the collection of prompt EL light. The optical chopper opens to collect the delayed EL at 0.3 ms after the forward bias is turned off. This is significantly longer than the typical lifetime of the triplet

excitons in phosphorescent emitter, which assures that the contribution of the generated excitons during the applied forward bias to the delayed EL is negligible. During the signal collection a reverse bias pulse width of 0.5 ms is applied on the devices to identify the effect of reverse bias on the delayed EL. Unlike in fluorescent OLEDs, any contributions from guest-guest TTA to the delayed EL in the milliseconds time frame, which is used in our measurements here, will be insignificant in case of PHOLEDs. This is due to the much shorter lifetime of phosphorescent guest triplet excitons due to the efficient intersystem crossing; thus, any such processes must occur over a much shorter time scale (i.e. << 1 ms).

In general, this delayed EL can be the product of one or several of the following processes: (i) recombination of trapped charges which are released after the end of the forward bias pulse; (ii) slow migration of host triplet excitons that are generated during the electrical excitation and their late arrival to the proximity of guest sites where energy transfer to the guest can take place; and (iii) TTA, which in this case will be primarily due to the fusion of host triplet excitons (i.e. host-host TTA. Processes (ii) and (iii) can generally be described by the following multi step mechanistic schemes:

Process ii:

$H_3^* + G_o \rightarrow H_o + G_3^*$ (Energy transfer) (ii-1)

$G_3^* \rightarrow G_o + h\nu$ (Phosphorescence) (ii-2)

Process iii:

$H_3^* + H_3^* \rightarrow H_1^* + H_o$ (Host-host TTA) (iii-1)

$H_1^* + G_o \rightarrow H_o + G_1^*$ (Energy transfer) (iii-2)

$G_1^* \rightarrow G_3^*$ (Intersection crossing) (iii-3)

$G_3 \rightarrow G_o + h\nu$ (Phosphorescence) (iii-4)

where H_1^*, H_3^*, G_1^*, G_3^*, H_o, and G_o denote host singlet exciton, host triplet exciton, guest singlet exciton, guest triplet exciton, host ground state, and guest ground state, respectively. Therefore, in order to differentiate between these processes, a 0.5 ms reverse bias pulse (of magnitude -0.5V) is applied on the devices during the delayed EL signal collection, and subsequent changes in delayed EL characteristics are monitored. Should the delayed EL be mainly the result of recombination of de-trapped charges (i.e. process i), such charges would be swept out of the EML by the reverse bias field, manifesting itself in a sudden and irreversible decrease in the delayed EL by the reverse bias pulse. Should, on the other hand, the delayed EL be primarily the result of TTA (i.e. process iii), then it would undergo only a temporary reversible decrease during the reverse bias pulse, and recover almost completely at the end of the pulse. Such temporary decrease in delayed EL is caused by the electric field-induced quenching of the host singlet H_1^* intermediate.

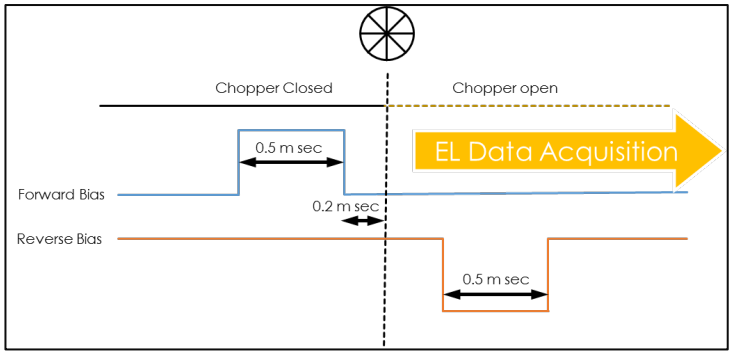

Figure 3.2 Delayed EL timing setup

Chapter Four: Explaining the Different Efficiency Behavior of PHOLEDs with/without a Hole Injection Barrier at the Hole Transport Layer/Emitter Layer Interface

In this chapter, the two emission mechanisms and their effects on the efficiency and efficiency roll-off will be investigated. Devices with and without a hole injection barrier will be studied. It will be shown that host e-h recombination leads to higher efficiencies than guest e-h recombination. In addition, host e-h recombination is associated with significant efficiency roll-off mainly due to the host-host TTA. This work has been published in Org. Electron., 10*,* **14***,* 2510-2517*,* 2013*. It has been reproduced with permission from the publisher under license number 3212910673067.*

4.1 Introduction

In general, PHOLEDs emission is a result of two mechanisms: i) e-h recombination on the guest molecules and ii) e-h recombination on the host followed by energy transfer to the guest. The former mechanism mainly arises from the charge trapping characteristics of the guest emitter in the host matrix. This is due to the fact that for a better exciton confinement on the guest emitter, guest molecules should have a narrower bandgap than host molecules. In this case, guest molecules can trap electrons and/or holes and form excitons [59,76]. On the other hand, the second mechanism was found to be the principal mechanism when charge trapping effect by the guest dopant is insignificant. It was shown that proper selection of a host: guest system with small difference between the bandgap of host and guest can significantly enhance this type of emission mechanism [77].

Guest concentration in the EML is one of the critical parameters that has to be carefully optimized in order to improve device efficiency. Several researches have been focused studying the performance behavior of the PHOLEDs with various guest concentrations [59,76,78-80]. It

was shown that the efficiency and efficiency roll-off of PHOLEDs varies significantly with the amount of guest concentration. Generally, efficiency of the PHOLEDs reduces significantly at high guest concentration. In this regard, optimum guest concentrations to achieve high efficiency are proposed. The general models proposed describing the low efficiency observed in devices with high guest concentrations are the presence of trapped charges on the guest and subsequent TPQ and quenching of triplet excitons by guest-guest TTA process, although the latter model does not explain the observed efficiency roll-off in devices with low guest concentrations. However, in a recently published study [79,81], efficiency behavior of devices with various guest concentrations is different in contrary to the previous study. The main difference between this device architecture and previously studied devices is the removal of hole injection barrier at the HTL/EML interface. Interestingly, efficiency and extend of efficiency roll-off in this device do not show significant dependency to the amount of guest concentrations opposing to the previously reported studies demonstrating direct influence of guest concentration to the device efficiency. In this work we investigate the different efficiency behaviors of the devices with and without hole injection barrier.

4.2 Result and discussion

Two series of devices, referred to as type A and Type B devices respectively, which differ from each other by the presence (series A) or absence (series B) of a hole injection barrier between the HTL and the host material of the EML are fabricated and studied. In each series $Ir(ppy)_3$ is doped at various concentrations in the EML. The devices have the following structures:

- Series A: ITO/MoO3(1nm)/NPB(40nm)/CBP: $Ir(ppy)_3$ (30nm)(100-x%,x%)/BAlq(10nm)/Alq3(30nm)/Mg:Ag

- Series B: ITO/MoO3(1nm)/CBP(35nm)/CBP: $Ir(ppy)_3$ (10nm)(100-x%,x%)/TPBI(40nm)/Mg:Ag

In these devices x represents the concentration of $Ir(ppy)_3$ in the EML. The electroluminescence characteristics of are summarized in Tables 4.1 and 4.2, respectively. Figure 4 shows the energy band diagrams of the devices. Figures 4.2a and 4.2b show the current efficiency versus current density of the same devices, respectively. As can be seen from the figures series A devices generally have lower efficiency, and their efficiency trends are more strongly influenced by $Ir(ppy)_3$ concentration. For example, the devices with 2% and 4% $Ir(ppy)_3$ (by volume) have a much higher efficiency at low currents, but at the same time display a larger efficiency roll-off in comparison to those with a higher guest concentration (i.e. 12%). In contrast, all series B devices show similar efficiency levels and trends irrespective of the guest concentration.

Table 4.1 Electroluminescence characteristics of the series A devices with various concentrations of Ir(ppy)3 at 20 mA/cm2 current density.

$Ir(ppy)_3$ concentrations (%)	Voltage (V)	Brightness (cd/m^2)	CIE
2	15.37	2500	0.311, 0.608
4	14.72	3500	0.321, 0.612
8	13.45	3590	0.330, 0.610
12	12.36	1930	0.337, 0.602

Table 4.2 Electroluminescence characteristics of the series B devices with various concentrations of $Ir(ppy)_3$ at 20 mA/cm^2 current density.

$Ir(ppy)_3$ concentrations (%)	Voltage (V)	Brightness (cd/m^2)	CIE
2	8	5950	0.337, 0.602
4	8.84	6700	0.338, 0.600
8	9	6900	0.345, 0.598
12	9.11	6200	0.344, 0.599

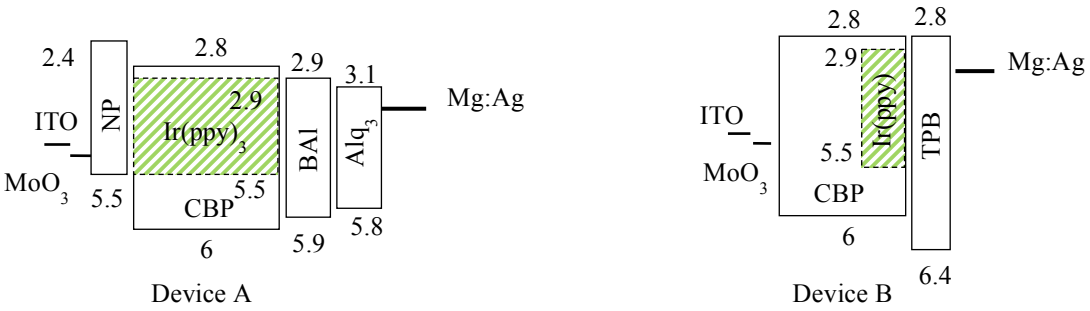

Figure 4.1 Energy band diagrams of the device A and B.

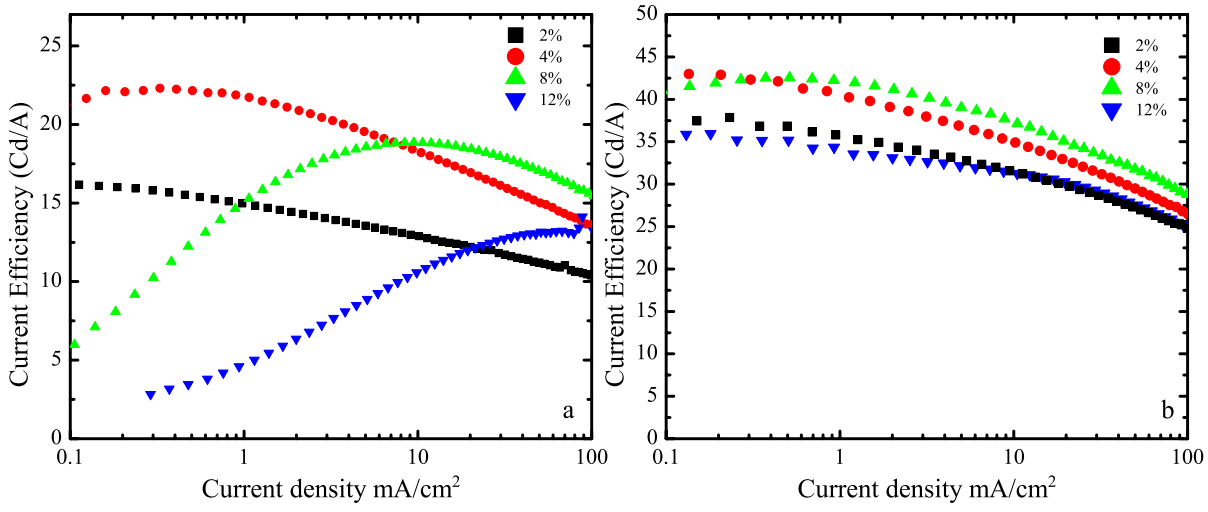

Figure 4.2 Current efficiency versus current density of devices a)A and b)B with various concentrations of $Ir(ppy)_3$.

In order to help understand the different dependence of the efficiency behavior on the guest concentration in the two types of devices, we studied the delayed electroluminescence (EL) characteristics from these devices using the previously reported technique [24]. Figures 4.3a and 4.3b show the normalized delayed EL intensity versus time (after the applied forward voltage corresponding to the 0.5 mA/cm^2 current density) under the applied reverse bias of series A and series B devices, respectively. Time 0 on the x-axis corresponds to 0.3 ms after the end of the forward bias pulse. It should be noted that spectral measurements show that the delayed EL corresponds to $Ir(ppy)_3$ emission.

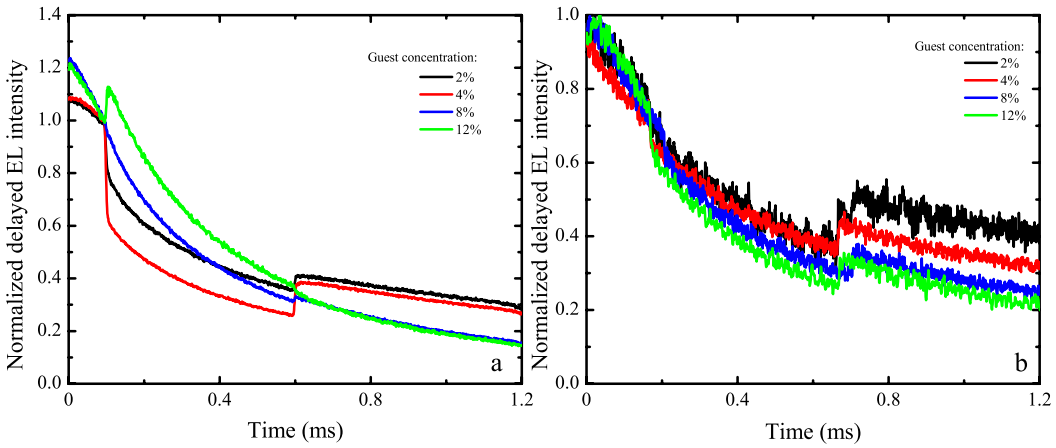

Figure 4.3 Normalized delayed EL intensity of devices a) A and b)B under the application of −2v reverse bias during signal collection.

Looking first at series A devices, delayed EL from devices with 2% and 4% Vol. $Ir(ppy)_3$ (figure 4.3a) show a sudden decrease of intensity under the application of reverse bias and recover completely at the end of the reverse bias. As a recovery at the end of the reverse bias indicates that host-host TTA is the primary source of delayed EL emission, it follows that a high concentration of host triplet excitons must be present in these devices. The high concentration of host excitons in these devices can be attributed to the fact that at low guest concentration only a very limited number of $Ir(ppy)_3$ sites will be available in the EML near the HTL/EML interface. Therefore, hole injection from the HTL into the EML will occur mostly unto CBP instead of $Ir(ppy)_3$ molecules. Therefore in these devices host e-h recombination and subsequent energy transfer to the guest will be the primary electroluminescence mechanism [82]. In contrast, the delayed EL characteristics of the devices with high guest concentrations (i.e. 8%>) do not show a similar recovery at the end of the reverse bias pulse, indicating that host-host TTA is not significant in this case, suggesting that guest e-h recombination as opposed to host e-h recombination is the dominant mechanism. This can be attributed to fact that the injection of holes from the HTL into the EML will occur unto $Ir(ppy)_3$ directly in these devices considering the lower injection barrier and the abundance of $Ir(ppy)_3$ sites at such concentrations (HOMO energy level of NPB is 5.5 eV and the HOMO levels of $Ir(ppy)_3$ and CBP are 5.5 eV and 6 eV, respectively [83]). Therefore, the creation of triplet excitons on the host becomes very limited, hence the limited host-host TTA in these devices. We also note the sudden increase in delayed EL intensity at the start of the reverse bias pulse in this case. The appearance of a spike can be attributed to residual charges which get redistributed under the influence of the reverse bias allowing for e-h recombination to occur, thus producing the sudden increase in delayed EL. The appearance of the spike therefore points to the presence of a significant number of residual

charges within the EML, which could possibly be residing (i.e. trapped) on the narrower band-gap guest molecules. The presence of a large number of charges (i.e. polarons) on $Ir(ppy)_3$ can cause significant quenching of excitons due to the TPQ [59,84]. In case of the device with 8% $Ir(ppy)_3$, we can see that applying a reverse bias pulse does not lead to a spike, suggesting that the number of trapped charges must be less in comparison to the device with higher guest concentration. Moreover, the delayed EL intensity decreases at the beginning of the reverse bias pulse then rebounds at the end of the pulse; an indication of host-host TTA. The magnitude of the decrease and the recovery were however smaller in comparison to those observed in devices with the lower guest concentrations, suggesting that host-host TTA is less. That an $Ir(ppy)_3$ concentration of ~8% generally gives the most optimum efficiency behavior in these PHOLEDs (according to figure 5.1a and also the large body of published work) [7,85-87]suggests that the optimal performance arises from an optimal balance between host e-h recombination and guest e-h recombination mechanisms. The higher efficiency of devices with lower (i.e. <8%) $Ir(ppy)_3$ at low driving currents (< 10 mA/cm2) indicates that host e-h recombination mechanism generally leads to a higher electroluminescence efficiency in comparison to guest e-h recombination and is therefore more favorable from a device efficiency standpoint.

Turning our attention now to series B devices, it can be seen from figure 4.3b that all devices show a recovery in delayed EL intensity at the end of the reverse bias, suggestive of host-host TTA in all devices, irrespective of the guest concentration. The observation suggests that unlike in series A devices, host e-h recombination is the dominant mechanism irrespective of the guest concentration in this case. This different behavior can be attributed to the absence of a hole injection barrier between the HTL and the host of the EML (both made of CBP) in series B devices, which allows holes to drift easily from the HTL to the EML where they continue to be

transported unto host sites, thus promoting host e-h recombination. As the injection of holes into the EML does not require assistance from $Ir(ppy)_3$ in this case, device efficiency is not dependent on guest concentration [79]. The generally higher efficiency of series B devices and of devices with no hole injection barrier at the HTL/EML interface in general [81] can perhaps be attributed to the fact that e-h recombination occurs mostly on the host, a route that, from our findings above, appears to lead to much higher electroluminescence efficiency in comparison to guest e-h recombination.

In order to further verify the correlation between device efficiency and a higher host versus guest e-h recombination, we include, in our comparison, a device where the HTL is made of TCTA (4,4',4"-tris(carbazol-9-yl)triphenylamine). As the HOMO energy of TCTA is 5.7eV, the hole injection barrier at the HTL/EML in this case will be ~0.3 eV, and therefore represents an intermediate case between type A devices (where the HTL is NPB and the barrier is highest, ~ 0.5eV) and type B devices (where the HTL is CBP and the barrier is lowest, ~0.0eV). As a higher barrier promotes the scenario where holes are injected directly unto guest molecules rather unto host molecules, the ratio of host e-h recombination to guest e-h recombination can be expected to decrease in the same direction (i.e. CBP → TCTA → NPB).

Figure 4.4 shows the current efficiency versus current density of the three devices (Structure: ITO/MoO3(1nm)/HTL(40nm)/CBP: $Ir(ppy)_3$ (30nm)(92%,8%)/TPBI(40nm)/Mg:Ag). As can be seen from the figure, the efficiency decreases as the hole injection barrier increases. supporting the notion that increasing the host e-h recombination /guest e-h recombination ratio leads to a higher device efficiency.

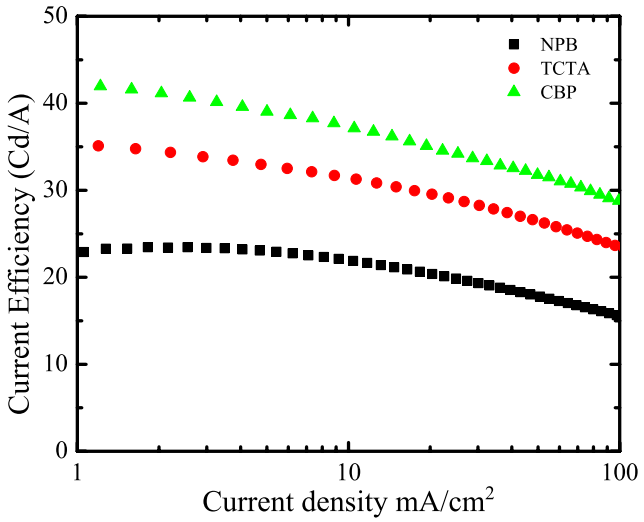

Figure 4.4 Current efficiency versus current density of devices with different HTLs.

As figure 4.2a shows that the devices with 2% and 4% Vol. $Ir(ppy)_3$ show much higher efficiency roll-off in comparison to the devices with 8% and 12% Vol. $Ir(ppy)_3$, the results imply that the higher efficiency roll-off may be associated with quenching of host excitons. In order to investigate this possibility, we study delayed EL from type A devices after driving at different forward bias magnitudes. Figures 4.5a, 4.5b, 4.5c and 4.5d show the delayed EL from devices with 2%, 4%, 8% and 12% $Ir(ppy)_3$, respectively. Figures 4.5a', 4.5', 4.5c' and 4.5d' show the effect of applying a -2V reverse bias on the delayed EL signal in each case. As figures 4.5a and 4.5b show, increasing the bias magnitude causes the decay rate of the subsequent delayed EL to become faster. The faster decay rate of delayed EL following a higher forward bias and the presence of the host-host TTA indicates that the TTA process is the primary source of host exciton quenching. Interestingly, for the device with 8% $Ir(ppy)_3$, the delayed EL decay rate does not change appreciably with the magnitude of the forward bias, suggesting that the quenching process does not increase with bias (and hence current) for this particular

concentration. At higher $Ir(ppy)_3$ concentrations (e.g. 12%) the delayed EL decay rate is faster when the bias the device was subjected to was higher (although only slightly this time). As $Ir(ppy)_3$ traps holes within the EML, the number of trapped holes generally increases with increasing the guest concentration [33] , a phenomenon that is also evident from the appearance of a spike in the delayed EL when a reverse bias is applied. The slightly faster decay rate of delayed EL may in this case be due to the quenching of host excitons by polarons on the guest sites via TPQ. The results suggest that the optimal performance observed at 8% is likely due to the fact that both host-host TTA and TPQ are minimum at this particular concentration. A close examination of the extent of the efficiency roll-off and the delayed EL results reveals a clear correlation between the host-host TTA and the efficiency roll-off suggesting that roll-off is primarily due to annihilation of host excitons. The fact that efficiency roll-off is relatively much lower in devices with high guest concentrations shows that guest-guest TTA plays a negligible role in comparison, consistent with previous conclusions [33].

Although host e-h recombination is the dominant mechanism in type B devices, they generally still exhibit lower efficiency roll-off in comparison to their type A counterparts for concentrations where host e-h recombination is the dominant mechanism in type A devices as well, such as at 2% and 4% $Ir(ppy)_3$. In order to understand the reasons behind the lower efficiency roll-off in type B devices, we studied delayed EL of devices A and B with 4% $Ir(ppy)_3$ concentration at low and high forward current densities (0.5 mA/cm^2 and 20 mA/cm^2, respectively). Figure 4.6 shows the delayed EL of these devices. As can be seen from the figure, applying a reverse bias pulse has almost identical effects on the delayed EL signals from the type

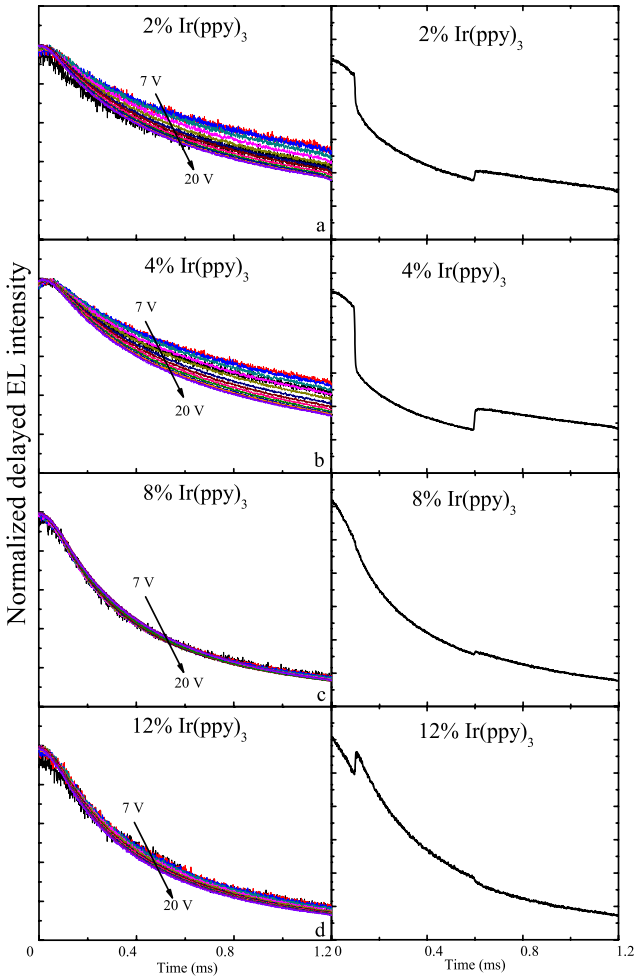

Figure 4.5 Delayed EL of devices A devices with a)2%, b)4%, c)8% and d)12% Vols. $Ir(ppy)_3$ concentrations at various forward biases.

A device, regardless of the magnitude of the forward bias current, suggesting that host-host TTA is similar at both current levels. In contrast, the delayed EL signals of type B device show different responses to the applied reverse bias at low and high current densities. For the case of 0.5 mA/cm^2 , the delayed EL shows the host-host TTA fingerprint (i.e. the recovery at the end of the reverse bias pulse) whereas for the case of 20 mA/cm^2 , the reverse bias pulse results in a sudden increase in delayed EL intensity appearing as a spike at the beginning of the pulse. We also see no detectable recovery in delayed EL at the end of the delayed EL (the recovery being the sign of host-host TTA as described above) , suggesting that host-host TTA is not significant

at high driving currents in these devices. The reduced host-host TTA and the appearance of a delayed EL spike at the beginning of the reverse bias are both suggestive of a wider e-h recombination zone in these devices especially at high current densities. A wider recombination zone would result in a lower exciton concentration per unit volume and hence reduced host-host TTA. At the same time, the overlap of electrons and holes over a wider region of the EML would result in the presence of residual charges (both electrons and holes) also over a wider region and thus a large number of e-h recombination events when a reverse bias is applied (causing the redistribution of these residual charges, and hence the delayed EL spike). The conclusion that type B devices have a wider e-h recombination zone versus devices A is of course entirely consistent and indeed expected considering that hole injection from the HTL to the EML is unrestricted in these devices, and therefore, unlike in type A devices, holes can easily penetrate across the EML. Therefore, host-host TTA is the primary source of the efficiency roll-off and the role of the guest-guest TTA on the efficiency roll-off is insignificant.

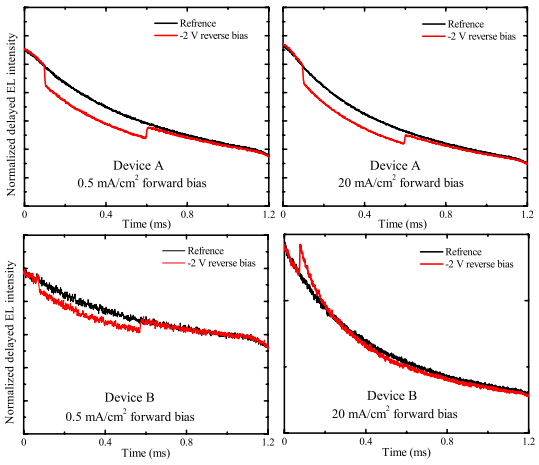

Figure 4.6 Delayed EL of devices A and B with 4% Vol. $Ir(ppy)_3$ concentration at the forward biases of 0.5 mA/cm^2 and 20 mA/cm^2 current densities

4.3 Summary

In summary, our results show that the recombination of electrons and holes on the host material generally leads to higher device efficiency in comparison to the case where recombination happens on the guest material. The results also show that in devices where a hole injection barrier between the hole transport layer (HTL) and the host material in the emitter layer (EML) exists, the emission mechanism gradually changes from one based on host e-h recombination to one based on guest e-h recombination as the guest concentration is increased. When host e-h recombination is dominant, although it tends to produce higher device efficiency, host e-h recombination is generally also associated with significant efficiency roll-off; the latter arises from quenching of the host triplet excitons primarily due to host-host TTA. As the concentration of the guest molecules increases and the creation of host triplet excitons subsides (since most e-h recombination occurs on the guest) host-host TTA decreases, hence also the efficiency roll-off. In such case, quenching is mostly caused by polarons residing on guest sites. At optimum guest concentrations (~8 % Vol.), a balance between host e-h recombination and guest e-h recombination is reached, and thus also minimal TTA and Triplet-Polaron Quenching. On the other hand, in devices where hole injection barrier between the HTL and the host in the EML is insignificant, emission mechanism is always based on host e-h recombination irrespective of the guest concentration, and therefore have higher efficiency and the efficiency does not depend on guest concentration. The absence of the injection barrier in these devices results in a wider recombination zone, and hence a lower exciton concentration in general, which in turn reduces host-host TTA and thus lowers efficiency roll-off In contrast, guest-guest TTA is not found to play a significant role in device efficiency behavior.

Chapter Five: Triplet-polaron Quenching by Charges on Guest Molecules in Phosphorescent Organic Light Emitting Devices

In this chapter, the underlying mechanisms associated with TPQ will be discussed. It will be shown that the efficiency loss due to TPQ is mainly caused by charges within the bulk of the EML rather than by charges in the HTL or at the HTL/EML interface. This work has been published in Appl. Phys. Lett., 6, **101**, 063502, 2012*. It has been reproduced with permission from the publisher under license number 3212910617869.*

5.1 Introduction

As was mentioned previously, one of the open issues in PHOLEDs is a decline in their efficiency at high current densities. TTA was believed to be the main reason for this behavior [61]. Then after, it was found that TPQ also plays a major role in this effect [32,33,58]. In this regard, poor charge balance in the device aggravates this effect. More recently, Wang *et al.* demonstrated a PHOLED with high efficiency and reduced roll-off efficiency, by means of using CBP for the HTL of the device, in addition to its utilization as the host material in the emitting layer [81]. The improvements were attributed to increased charge balance and the elimination of abrupt changes in HOMO levels across the HTL/EML interface. Their findings suggested that the stronger quenching in other devices must be primarily caused by charges that accumulate in the HTL or at the HTL/EML interface as a result of the interfacial hole injection barrier. Other results however suggested that the TPQ is caused mostly by charges within the EML bulk. As such, the nature of the underlying polaronic species and their location within the device remain unclear, making it difficult to devise approaches to reduce them and improve device efficiency.

5.2 Result and discussion

First, to determine the width of the electron-hole (e-h) recombination zone (i.e. where excitons are formed), and how far it extends into the EML layer away from the HTL/EML (i.e. where the majority of TPQ presumably occurs), we study a series of devices of the following structure: ITO/MoO_3 (10 nm)/ NPB (40 nm)/CBP:$Ir(ppy)_3$ (92%/8%) (x nm)/CBP(40-x nm)/BAlq (10 nm)/Alq_3 (30 nm)/Mg:Ag. Their EL characteristics are summarized in Table 5.1. Clearly, reducing the thickness of the $Ir(ppy)_3$-doped CBP layer from 40 nm to 20 nm does not bring about significant changes in device brightness or efficiency, indicating that the majority of e-h recombination occurs within 20 nm from the HTL/EML interface. In order to obtain some insights about exciton and charge distributions in the recombination zone region, we conduct delayed EL measurements on the same devices. In this technique, the devices are driven with a 0.5 ms width square pulse forward bias, and persistent (delayed) EL is collected ~0.3ms after the end of the forward bias pulse, using an optical chopper system [24,88,89]. This delay time which is significantly longer than the lifetime of $Ir(ppy)_3$ triplet state lifetime (<1 μs) is selected to ensure the absence of any contributions from prompt EL in the collected signal. As such, any collected signal will arise from radiative decay of excitons that are formed after the bias is turned off.

Table 5.1 Electroluminescence characteristics of the devices with various thicknesses of doped region at 20 mA/cm2 current density.

X (nm)	Voltage (V)	Brightness (cd/m^2)	CIE
40	13.31	3140	0.343, 0.598
30	14.61	3170	0.343, 0.597
20	14.59	2980	0.344, 0.596
10	14.74	1770	0.347, 0.586

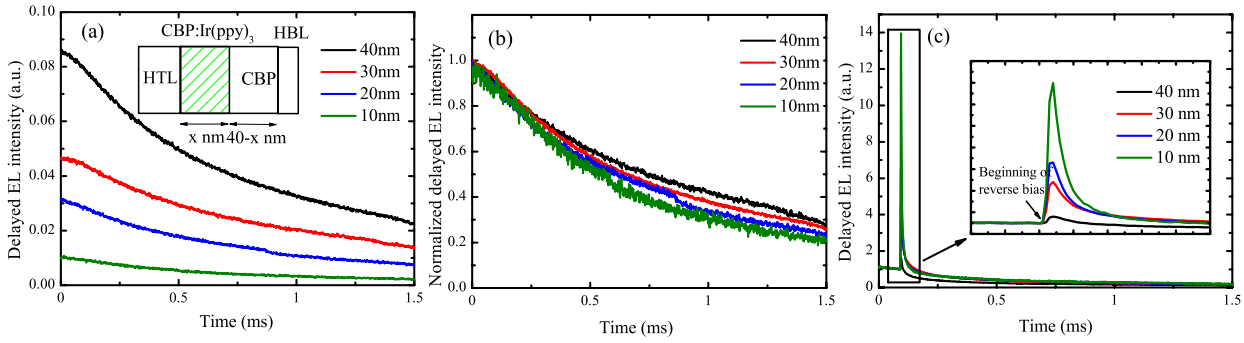

Figure 5.1 a) Delayed EL intensity, b) normalized delayed EL intensity and c) delayed EL intensity under -5 V reverse bias of the devices with various thicknesses of Ir(ppy)$_3$-doped layer. Time 0 on the x-axis corresponds to time that the optical shutter opens.

Figure 5.1a shows the relative intensity of delayed EL collected from these devices versus time. Time 0 on the x-axis corresponds to the time the optical shutter opens. Spectral measurements show that the delayed EL emission corresponds to Ir(ppy)$_3$ emission (data not shown here in the interest of brevity). Unlike in case of prompt EL intensity which varies very little on reducing the thickness of the Ir(ppy)$_3$-doped layer from 40 nm to 20nm (the data in table 5.1), the delayed EL intensity decreases by about 60%. This decrease in delayed EL intensity can be attributed to a decrease in the formation of CBP triplets as direct e-h recombination on Ir(ppy)$_3$ guest molecules, rather than on CBP host molecules, increasingly becomes the dominant emission mechanism as we move closer the HTL/EML interface [90]. Figure 5.1b shows the same delayed EL data after normalizing to the same initial intensity. Despite the small differences, the decay rate of delayed EL becomes visibly faster as the doped layer becomes thinner. The faster decay is suggestive of an increased quenching of triplet excitons on CBP, which otherwise would have been transferred to Ir(ppy)$_3$ and contributed to the delayed EL. To further investigate this behavior, we study the effect of applying a reverse bias pulse (of -5V magnitude) on the delayed EL characteristics. Figure 5.1c displays the delayed EL characteristics

in this case. As can be seen from the figure, the application of a reverse bias pulse results in a sudden increase in the delayed EL intensity. The delayed EL spike points to the presence of a high concentration of residual (i.e. accumulated) charges in the EML. These charges get redistributed by the reverse bias, leading to the sudden increase in e-h recombination events [91]. Figure 4.1c inset shows the relative magnitudes of the delayed EL spikes among the devices (by normalizing to the same delayed EL intensity just prior to the application of the reverse bias pulse). As can be seen from the figure, the relative magnitude of the spike increases when the thickness of the $Ir(ppy)_3$-doped layer is decreased, indicating that the relative concentration of residual charges increases in the same direction. The fact that the devices with the thinner doped region have relatively higher concentrations of residual charges further supports the notion that e-h recombination occurs directly on the guest (rather than on the host) in the vicinity of the HTL/EML interface, leading to the higher concentration of trapped residual charges on the narrower band-gap guest. On the other hand, as the distance from the interface increases, e-h recombination occurs more increasingly on the host. The faster decay rate of delayed EL observed in case of thinner doped layers (of figure 5.1b) can therefore indeed be due to increased exciton quenching by the higher concentration of residual charges on $Ir(ppy)_3$ sites in the EML, close to the HTL. The results therefore suggest that the TPQ is mostly caused by charges within the EML, and is more severe in the region adjacent to the HTL/EML interface.

Although the above results suggest that residual charges on $Ir(ppy)_3$ within the EML in the vicinity of the HTL/EML interface play a major role in the TPQ process, it is possible that residual charges in the HTL or at the HTL/EML interface, which may accumulate due to the presence of a hole injection barrier at the interface, also contribute significantly to the quenching process[60]. In order to investigate this possibility, we study a series of devices with various

$Ir(ppy)_3$ concentrations. The general device structure is: ITO/MoO3 (10 nm)/ NPB (40 nm) /CBP:$Ir(ppy)_3$ (100-y% : y%) (40 nm)/BAlq (10 nm)/Alq_3 (30 nm)/Mg:Ag. (where y represents the volume fraction of $Ir(ppy)_3$). As the HOMO energy level of CBP is significantly deeper than that of NPB (6.0 eV and 5.46 eV, for CBP and NPB, respectively [14,15]), whereas the HOMOs of $Ir(ppy)_3$ and NPB are comparable (~5.3 eV for $Ir(ppy)_3$) [13], hole injection across the HTL/EML interface is known to occur mostly via injection from NPB unto $Ir(ppy)_3$ directly[92]. Therefore, increasing the concentration of $Ir(ppy)_3$ molecules can be expected to facilitate hole injection from NPB into the EML, and hence reduce possible hole space charges within the HTL or at the HTL/EML interface. Table 5.2 summarizes the EL characteristics of these devices. As expected, increasing the $Ir(ppy)_3$ concentration results in a decrease in device driving voltage, consistent with the guest's role in facilitating hole injection.

Table 5.2 Electroluminescence characteristic of devices with various concentrations of $Ir(ppy)_3$ dopants at 20 mA/cm^2 current density.

$Ir(ppy)_3$ concentration (%)	Voltage (V)	Brightness (cd/m^2)	CIE
2	15.37	2550	0.311, 0.608
4	14.72	3410	0.321, 0.612
8	13.45	3590	0.330, 0.612
12	12.36	1930	0.337, 0.602
16	11.87	1040	0.339, 0.590

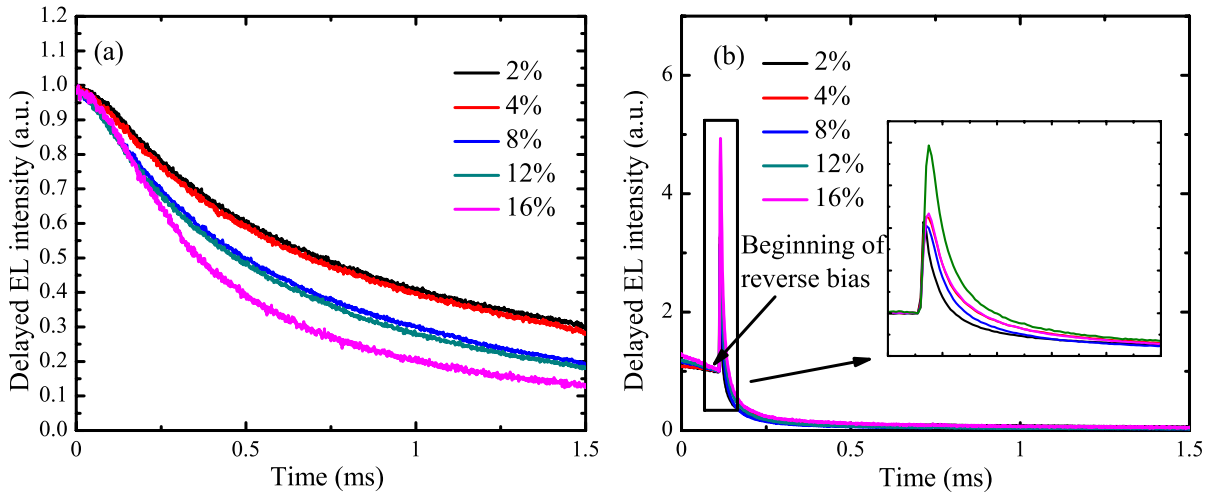

Figure 5.2 a) Normalized delayed EL intensity and b)delayed EL intensity under -5 V reverse bias of the devices with various concentrations of Ir(ppy)$_3$. Time 0 on the x-axis corresponds to time that the optical shutter opens.

Figure 5.2a shows the normalized delayed EL intensity of the same devices. Clearly, the decay rate of delayed EL becomes faster as the Ir(ppy)$_3$ concentration increases, suggestive of an increase in exciton quenching in the same direction. That the quenching is less in devices with expectedly higher hole space charge densities in the HTLs (i.e. devices with lower Ir(ppy)$_3$ concentration, hence more difficult hole injection from the HTL to EML) indicates that the quenching cannot be primarily caused by interfacial charges or space charges in the HTL. Figure 5.2b shows the effect of applying a -5 V reverse bias pulse on the delayed EL of these devices. Clearly, the height of the delayed EL spike increases on increasing the Ir(ppy)$_3$ concentration, pointing to an increase in the number of residual charges in the EML in the same direction. That both the quenching effect and number of residual charges increases as Ir(ppy)$_3$ concentration is increased further proves that the TPQ mechanism is indeed caused primarily by charges (holes) on Ir(ppy)$_3$.

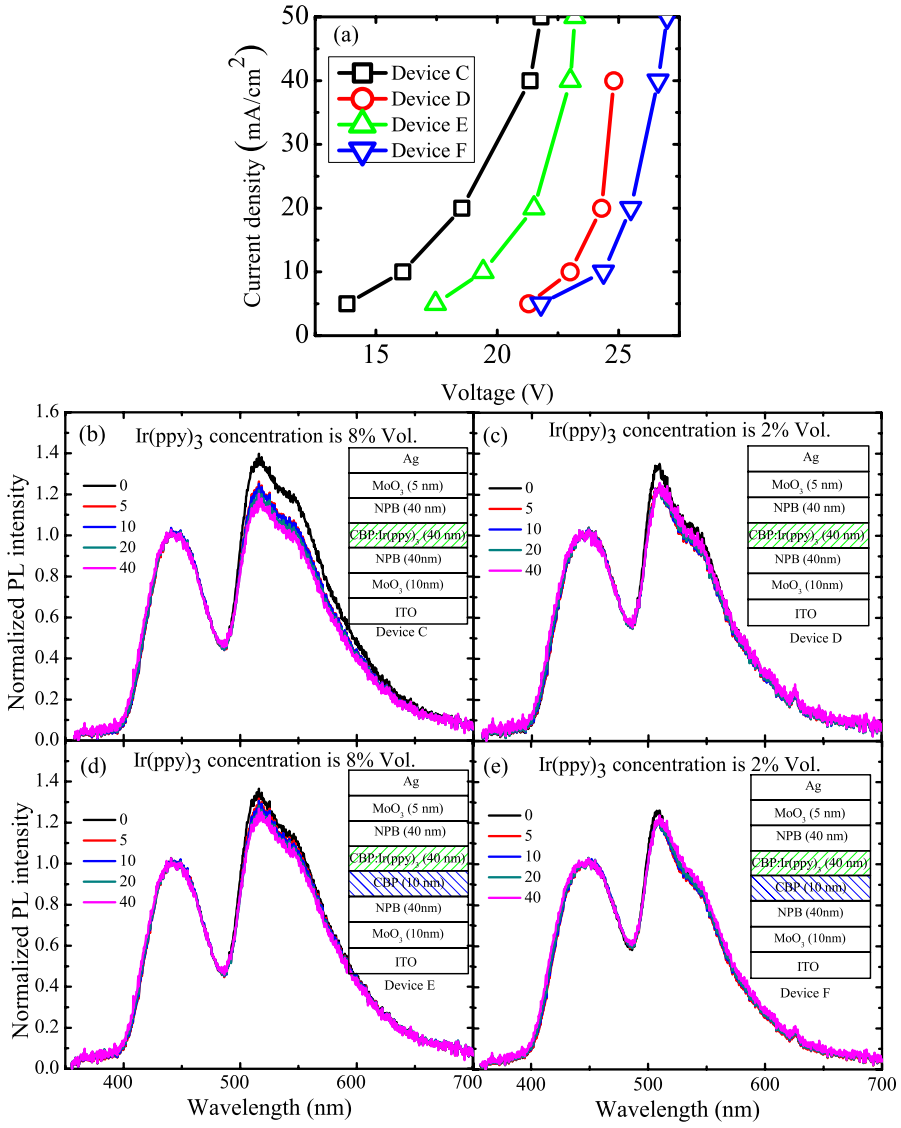

Figure 5.3 PL spectra of devices a)C, b)D, c)E and d)F excited at 290 nm excitation wavelength at various current densities (mA/cm^2).

To further verify the above notions, PL measurements on hole-only devices (i.e. devices where current flow under external bias proceeds predominantly by the transport of holes) that contain CBP:Ir(ppy)$_3$ layers with 8% or 2% Ir(ppy)$_3$ (denoted to as devices C and D, respectively), by volume, sandwiched between two NPB HTLs, are carried out. The general device structure is ITO/ MoO_3 (10 nm)/ NPB (40 nm)/CBP:Ir(ppy)$_3$ (40nm) /NPB(40nm)/MoO_3

(5nm)/Ag(100nm). The 10 nm MoO_3 layer is used to facilitate hole injection from the ITO unto the organic stack, whereas the 5 nm MoO_3 layer is used as an electron-blocking layer to minimize electron injection from Ag. As the concentration of $Ir(ppy)_3$ is higher in case of device C, one would expect the injection of holes into the CBP:$Ir(ppy)_3$ from the first NPB layer and hence also their flow across the organic layer stack to be easier in comparison to that in case of device D, and as a result, any buildup of hole space charges in the first NPB layer would also be lower in this case. Under forward bias (defined as ITO being at a more positive potential versus Ag), the driving voltage for 20 mA/cm^2 current density is found to be 18.54 V and 24.3 V for devices C and D, respectively, proving that the transport of holes is indeed easier in case of device C. It should also be noted that the devices show no detectable EL emission, indicating that current flow is indeed unipolar (i.e. hole only). Figures 5.3a and 5.3b show PL spectra from the two devices, respectively, under 290 nm excitation (where CBP absorbs significantly), and at various hole current densities. The PL spectra show two main emission bands with peaks at 440nm and 510nm, which correspond to emission from NPB and $Ir(ppy)_3$, respectively, the latter representing PL from the CBP:$Ir(ppy)_3$ layer. In order to facilitate comparisons between the relative PL intensities from the CBP: $Ir(ppy)_3$ layer under the various magnitudes, the spectra are normalized to the same NPB emission intensity. A comparison between figures 5.3a and 5.3b shows that increasing the current leads to a larger decrease in the PL intensity from the CBP: $Ir(ppy)_3$ layer in case of device C, signifying a larger decrease in its PL yield. The larger decrease in the PL yield of the CBP: $Ir(ppy)_3$ in this device, despite the fact that hole space charges in the first NPB layer in the vicinity of the NPB/CBP:$Ir(ppy)_3$ must be lower versus that in device D (due to the easier hole injection and transport into the CBP:$Ir(ppy)_3$ layer in this device) proves that the quenching effect must be caused by holes within the CBP:$Ir(ppy)_3$ layer

and not by holes in the NPB layer or at the NPB/CBP:$Ir(ppy)_3$ interface. Furthermore, as in device C the majority of holes are injected and subsequently transported into the CBP:$Ir(ppy)_3$ unto $Ir(ppy)_3$ molecules rather than on CBP molecules, whereas in case of device D a larger fraction of holes is transported on CBP molecules (due to the lower $Ir(ppy)_3$ concentration), it follows from the larger decrease in PL yield in case of device C that holes on guest molecules (versus holes on host molecules) are more effective in quenching excitons. In fact, PL measurements on hole-only devices that further include a neat CBP layer in-between the first NPB layer and the CBP:$Ir(ppy)_3$ layer show that the CBP:$Ir(ppy)_3$ PL intensity does not decrease significantly on increasing current in this case (figures 5.3c and 5.3d), indeed supporting the above argument. As in these devices the flow of current requires that holes must be injected from NPB into a neat CBP layer first (i.e. before reaching the CBP:$Ir(ppy)_3$ layer), and, as such, must surmount the large hole injection barrier at the NPB/CBP interface anyway, the majority of holes will continue to be transported on CBP sites within the CBP:$Ir(ppy)_3$ layer. Therefore, the concentration of holes on $Ir(ppy)_3$ sites in these devices will be much lower, regardless of the $Ir(ppy)_3$ concentration. Thus, in this case, increasing the current density brings about only a very limited increase in the TPQ process. The results therefore prove that holes (polarons) on the guest material are much more effective in quenching excitons and inducing the TPQ process in comparison to holes (polarons) on the host. These results perhaps also explain the lower efficiency roll-off observed in the devices by Wang *et al.* [81] In their devices, using a CBP HTL allows the majority of holes to be injected and transported on host rather than on guest sites in the EML. As a result, the concentration of the highly quenching guest polaronic species is much lower, hence the higher device efficiency and lower efficiency roll-off. In this regard, using other HTL materials with sufficiently deep HOMO levels so that hole injection from the

HTL to the host can proceed efficiently would reduce the concentration of holes on the guest material and, as a result, improve device efficiency. This may in fact be the reason, at least in part, for the higher efficiency and lower efficiency roll-off in devices utilizing TCTA (4,4',4"-tri(N-carbazolyl) triphenylamine) instead of NPB as an HTL [13]. Furthermore, from the same standpoint, a PHOLED design where e-h recombination occurs primarily on the host rather than on the guest can be expected to be beneficial for efficiency, as in the latter case, the concentration of charges on the guest will inevitably be significant.

5.3 Summary

In summary, results from delayed EL and PL measurements show that the efficiency loss due to TPQ is mainly caused by charges within the bulk of the EML rather than by charges in the HTL or at the HTL/EML interface. Charges on the guest rather than those on the host are found to be the most efficient in quenching excitons, revealing that guest polaronic species are the most detrimental to device efficiency. The results also show that direct injection of holes from the HTL into the guest material reduces device efficiency, suggesting that, for higher device efficiency, an emission mechanism based on e-h recombination on the host rather than the guest is more favorable.

Chapter Six: Luminescence Degradation in Phosphorescent Organic Light-Emitting Devices by Hole Space Charges

In this chapter, the effect of TPQ on the device operational stability will be discussed. It will be shown that formation of space charge at the EML/HBL interface significantly reduces the EL stability. Results from the delayed EL measurements further show that the loss of electroluminescence efficiency of PHOLEDs is due to a gradual increase in deep traps with electrical driving, which facilitates exciton quenching. This work has been published in J. Appl. Phys., 4, **109**, 044501, 2011. *It has been reproduced with permission from the publisher under license number 3212910318766.*

6.1 Introduction:

Along with efficiency roll-off, the other technical issue of PHOLEDs is their insufficient operational stability, which limits a wide commercialization of this technology [41,70]. Intensive research work focusing on the issue of electroluminescence degradation in organic light-emitting devices has been conducted [20,37,66-68,71] with the purpose of providing a comprehensive understanding of device degradation mechanisms. In reviewing these works, it appears that most of the studies focused on devices based on fluorescent emitters, whereas studies on devices based on phosphorescent emitters, i.e. PHOLEDs, have been limited. As PHOLEDs employ different emitting materials and generally have different device structures [10] from their fluorescent emitters-based counterparts, their failure can be expected to be caused by different degradation mechanisms. A better understanding of degradation mechanisms in PHOLEDs is therefore needed, and will be instrumental for guiding the efforts towards realizing more stable PHOLEDs.

Recently, Giebink *et al* identified exciton-polaron annihilation as a principal defect formation route in PHOLEDs [41]. It was proposed that energy transfer from an exciton to a polaron leaves a vibrationally hot, charged molecule, which is at a greater risk of bond cleavage due to the excess energy that must be dissipated. By using a unipolar device (a device that transports only holes or electrons), they experimentally showed that host anions of the emitting layer were unstable, and attributed it to energy transfer from guest excitons to host polarons [23]. However, they also found that the photoluminescence (PL) efficiency of the emitting layer in a unipolar device remained unchanged during electrical aging, an observation that cannot be fully explained by the exciton-polaron annihilation degradation model alone.

6.2 Results and discussion

In PHOLEDs, it is customary to include HBLs, layers that confine holes (and excitons) to the emitting layer and prevent them from reaching the ETL, with the purpose of increasing device efficiency [93]. Nevertheless, devices with a HBL usually have a lower stability than their counterparts [71] without a HBL. Figure 6.1 shows the normalized EL efficiency versus driving time of two PHOLEDs with and without HBL, where the devices are operated at a current density of 20 mA/cm^2. The HBL is made of BCP, a widely used material for that purpose. The layer structures of these two devices are:

ITO/NPB (50nm)/CBP:Ir(ppy)$_3$ (92%:8%, 40nm)/Alq$_3$ (30nm)/Mg:Ag (9:1, 100nm). (referred to as “Without HBL”)

ITO/NPB(50nm)/CBP:Ir(ppy)$_3$ (92%:8%, 40nm)/BCP(10nm)/Alq$_3$ (30nm)/Mg:Ag (9:1, 100nm).(referred to as “With HBL”)

As shown in the figure, the device with the HBL has a lower stability, evident in the more rapid decrease in its EL efficiency with time, in agreement with other reports [71]. We note that the observed stability is similar to that reported by some groups for the same device structure [94,95] but lower in comparison to other reports [96]. The wide variation in stability can be attributed to variations in ITO [18] and organic materials obtained from different suppliers. In our case, the materials are purchased from the Luminescence Technology Corp. and are used as received.

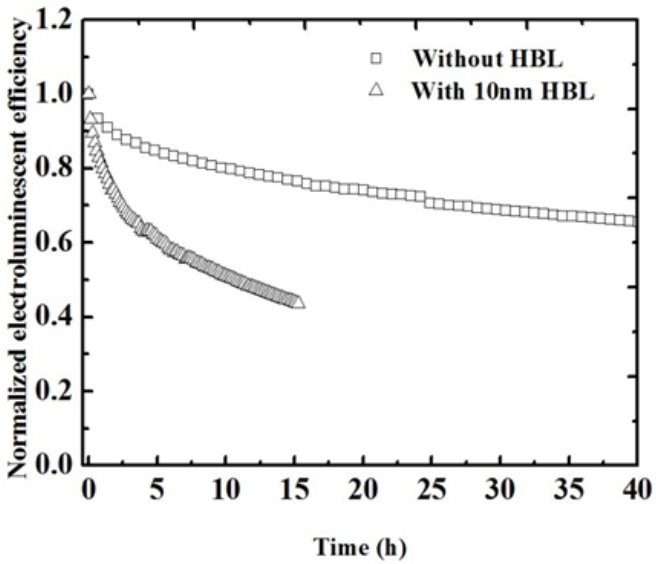

Figure 6.1 Normalized electroluminescent efficiency versus time of two typical PHOLEDs with and without BCP hole blocking layer.

To investigate the role of HBL on PHOLED degradation, a series of PHOLEDs of various structures, as schematically illustrated in Figure 6.2, are tested. In these devices, a DCJTB (4-(dicyanomethylene)-2-tert-butyl-6-(1,1,7,7-tetramethyljulolidin-4-yl-vinyl)-4H-pyran)-doped sensor layer is inserted at various locations. The driving voltage and EL intensity of these devices at 20 mA/cm^2 are given in Table 6.1. The very low luminance intensity of devices G and I can be attributed to the diffusion of triplet excited states into Alq_3, whereas the higher EL efficiency of devices H and J is due to exciton and hole confinement in the emitting layer by the HBL [71,97,98]. Figure 6.3 shows the EL spectra from the same devices. As can be seen from the figure, the spectrum from device G, in which the sensor layer is located in the ETL adjacent to its interface with the emitting layer, is somewhat broader in the 575-650 nm range, indicating more emission from the DCJTB sensor layer. In device H, on the other hand, the presence of the HBL leads to confinement of excitons and holes to the emitting layer, resulting in negligible emission from the sensor layer; consistent with previous reports [71,98]. In case of devices I and J, which are identical to devices G and H except that the sensor layers are located in the emitting layers instead of the ETLs, the spectra show very significant red emission component, corresponding to emission from DCJTB in the sensor layers, in addition to the $Ir(ppy)_3$ characteristic emission band at ~510nm. The strong emission from the sensor layer indicates that significant electron-hole recombination occurs at (or near) the electron injection interface of the emitting layer, contrary to some earlier reports [99]. A comparison between spectra from devices I and J shows higher $Ir(ppy)_3$/DCJTB emission ratio when a HBL is used (i.e. in case of device J), suggesting a shift in the recombination zone towards the middle of the emission layer, away from the sensor layer, and points to a shallower penetration of holes across the layer. The observation alludes to possible build-up of a hole space charge when an HBL is used, which

makes the transport of holes across the emitting layer more difficult. As the accumulation of space charges has been proven to be detrimental to the luminescence efficiency of fluorescent materials [66], it is possible that they have a similar effect on phosphorescent materials, and thus are behind the faster degradation of electroluminescence efficiency of PHOLEDs with HBL (Figure 6.1).

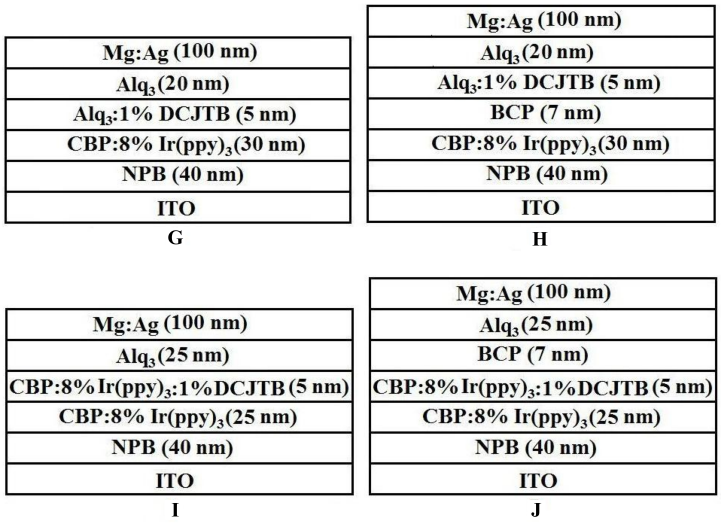

Figure 6.2. Schematic diagrams of the structure of devices G to J.

Table 6.1 Electroluminescence characteristics of devices G to J at a driving current density of 20 mA/cm2.

Sample	Voltage (V)	Luminance intensity (Cd/m2)	CIE color coordinates
(G)	10.8	1650	0.371 0.576
(H)	10.9	4700	0.336 0.606
(I)	10.7	700	0.461 0.510
(J)	11.3	2300	0.419 0.545

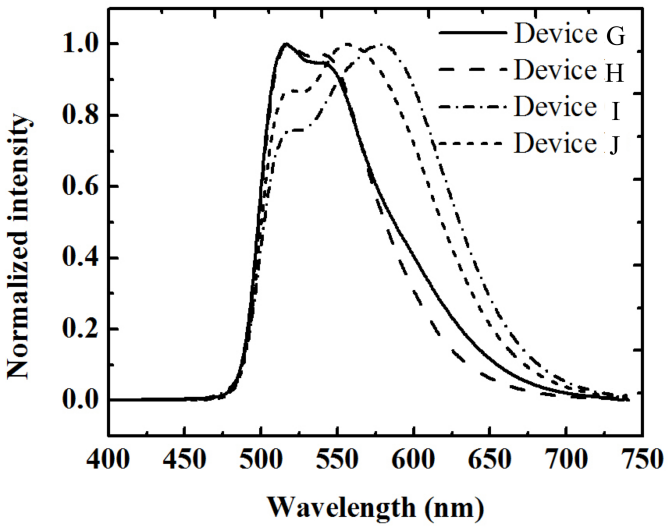

Figure 6.3 EL spectra of devices G, H, I and J measured before aging.

In order to explore this possibility, photoluminescence (PL) measurements on devices G and H are carried out. In these measurements, changes in device photoluminescence spectra under 440 nm excitation (at which only $Ir(ppy)_3$ and Alq_3 can be excited) after different periods of electrical driving (i.e. electrical aging) at constant current density of 20 mA/cm^2 are recorded. Figure 6.4 shows the normalized PL spectra of device G after 0, 20 and 40 hours of electrical aging. For reference, the non-normalized spectra are also shown in the figure (in the inset). As can be seen from the figure, the spectra show two main emission bands with peaks at 510 nm and 620 nm, which correspond to emission from $Ir(ppy)_3$ and DCJTB, respectively. We note that the spectra do not reveal an obvious emission from Alq_3. This can be attributed to the limited thickness of the Alq_3 layer, which causes the majority of the Alq_3 excitons to be either quenched by the metal cathode, or transferred to DCJTB molecules in the sensor layer through Forster energy transfer. As can be seen from the inset of Figure 6.4, the intensity of both emission peaks decreases with electrical aging, indicating a decrease in the PL efficiency of both the main emitting layer and the sensor layer. The normalized spectra, however, show that the PL intensity

of the sensor layer is decreasing faster, which points to a faster degradation of PL efficiency of the sensor layer as a result of electrical aging. The faster degradation of the sensor layer can be well explained by the Alq_3 cationic model [20]. In that model, cationic Alq_3 species is unstable and their degradation produces exciton quenchers that lead to a decrease in Alq_3 luminescence efficiency. In case of the PHOLEDs studied here, Alq_3 is used as an ETL rather than as an emitting layer. Therefore, the degradation of Alq_3 should not directly contribute to the quenching of excitons in the emitting layer. However, the degradation of the ETL can be expected to reduce its electron transport capacity. This, in turn, will alter the balance in hole/electron injection in the emitting layer, leading to a decrease in the luminescence efficiency of the PHOLEDs.

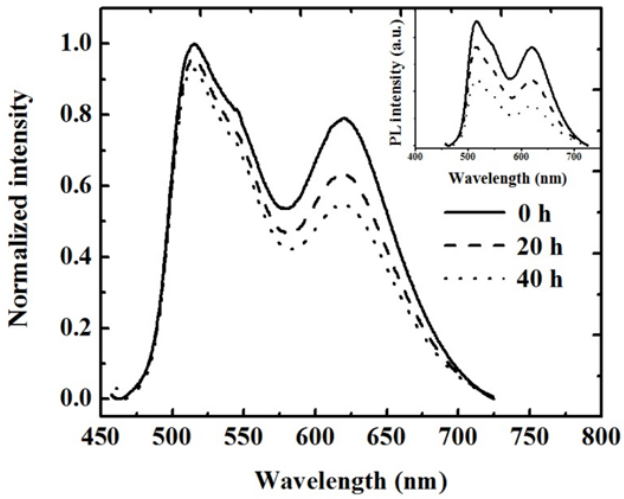

Figure 6.4 Normalized PL spectra of device G collected after aging for 0, 20 and 40 hours. Aging is done at a constant current density of 20 mA/cm^2.

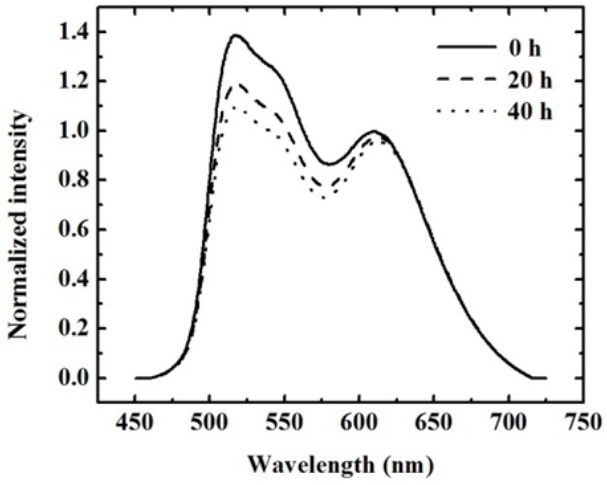

Figure 6.5 PL spectra of device H collected after aging for 0, 20 and 40 hours. Aging is done at a constant current density of 20 mA/cm^2.

Figure 6.5 shows the normalized PL spectra of device H, also collected after 0, 20 and 40 hours of electrical aging. Unlike in case of device G, the decrease in PL from the sensor layer is found to be slower than that from the bulk emitting layer, suggesting that electrical aging has different effects in devices G and H. As the hole mobility of NPB is two orders of magnitude higher than the electron mobility of Alq_3, the transport of holes to the emitting layer is much easier. As their leakage to the ETL is substantially reduced by the HBL, holes will gradually accumulate in the emitting layer, forming hole space charges [20,66]. The build-up of these space charges can result in a loss in the luminescence efficiency of the material, which can also be irreversible, thus lead to device electroluminescence degradation.

To verify this hypothesis, we use delayed EL measurements to investigate the effect of using a HBL on space charges in the emitting layer of PHOLEDs. Figures 6.6a and 6.6b show delayed EL signal from devices without and with a HBL, respectively, (the devices structures are: ITO/NPB (50nm)/CBP:Ir(ppy)$_3$ (92%:8%, 40nm)/Alq$_3$ (30nm)/Mg:Ag (100nm), and ITO/NPB (50nm)/CBP:Ir(ppy)$_3$ (92%:8%, 40nm)/BCP (10nm)/Alq$_3$ (30nm)/Mg:Ag (100nm), respectively. In each case, delayed EL is collected from the fresh device, and again from the same device after it has been electrically aged for 20 hrs at 20 mA/cm^2. As can be seen from the figure, the application of the reverse bias results in the appearance of a spike in delayed EL signal, which is an indicator of a sudden release of trapped charges that then recombine to produce the delayed EL [100]. The redistribution of some of these released charges when the reverse bias ends create a second opportunity for recombination, hence another (smaller) spike at the end of the pulse. In comparison to the device without HBL (Figure 6.6a), the device with the HBL (Figure 6.6b) shows higher spikes, indicating a higher concentration of trapped charges. This result is consistent with the supposition arrived to earlier from results in Figure 6.3 that the presence of a HBL leads to increased hole space charges in the emitting layer, hence also a higher concentration of trapped holes[71]. In the absence of a HBL, on the other hand, a large fraction of these holes can leak through to the ETL [101], hence the concentration of trapped holes is lower. More notably, figure 6.6 also shows a much larger increase in the magnitude of the delayed EL spikes from the device with the HBL after aging, revealing that the prolonged electrical driving leads to a much larger increase in the concentration of trapped holes in this case. The higher initial concentration of trapped charges in this device and the larger increase in their concentration upon electrical aging suggest they may be behind the lower stability of this device (from Figure 6.1).

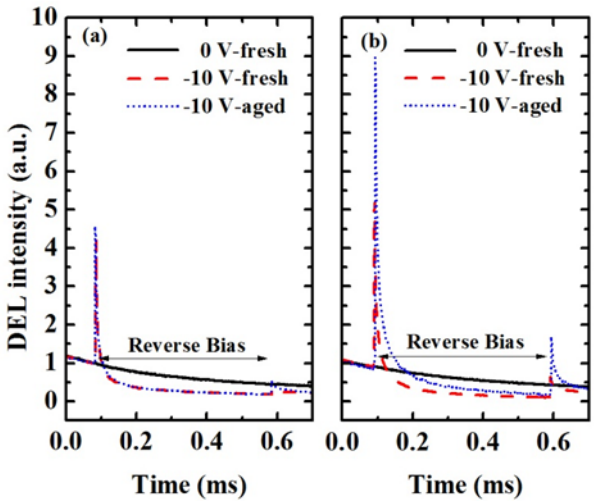

Figure 6.6 Delayed EL intensity versus time from devices of structure (a)ITO/NPB (50 nm)/CBP:Ir(ppy)3 (40 nm)/Alq3 (30nm)/Mg:Ag, and (b) ITO/NPB (50 nm)/CBP:Ir(ppy)3 (40 nm)/BCP (10 nm)/Alq3 (30 nm)/Mg:Ag, collected before (fresh) and after aging (aged) for 20 hours at 20 mA/cm2. During data collection, a 0.5 ms reverse bias pulse of magnitude -10V is applied (pulse interval denoted by arrows). Delayed EL from a fresh sample without the reverse bias is included for reference.

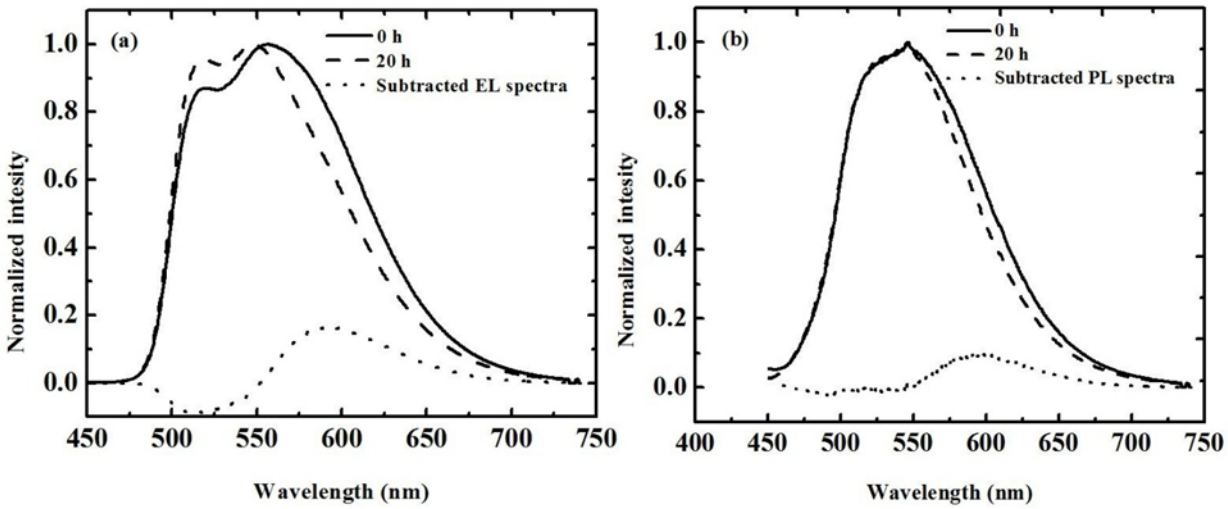

Figure 6.7 a) EL and b) PL spectra of device J collected after aging for 0 and 20 hours at a constant current density of 20 mA/cm2. The lower curves represent the mathematical difference between the spectra in each case.

To verify whether the trapped holes are indeed responsible for the faster degradation of the devices with a HBL, comparative PL and EL spectral measurements are carried out. Figure 6.7a shows normalized EL spectra from a device of structure J collected before and after aging for 20

hours at 20mA/cm^2, revealing a spectral shift in the spectra. The mathematical difference in the spectra (calculated by subtracting the final spectrum from the initial spectrum) corresponds to a spectrum with a peak wavelength of 600 nm (shown in figure 6.7a), which matches DCJTB emission from the sensor layer, indicating that the spectral shift is due to a decrease in the DCJTB/ $Ir(ppy)_3$ emission ratio after aging. Normalized PL spectra from the same device (Figure 6.7b) also display a small decrease in emission intensity on the long wavelength side of the peak after aging. The mathematical difference in the PL spectra corresponds to a spectrum with a peak wavelength of 600 nm (also shown in figure 6.7b), which again matches DCJTB emission from the sensor layer. We can, therefore, conclude that the photoluminescence yield of the sensor layer degrades faster than that of the bulk of the emitting layer. The similar trends in EL and PL therefore suggest that the faster degradation of electroluminescence from the sensor layer versus that from the bulk of the emitting layer (figure 6.7a) is due to a faster loss in its luminescence quantum yield. In principle, there are two possible mechanisms for the faster degradation of the sensor layer in device J: (i) the doping of DCJTB accelerates the degradation of the sensor layer perhaps due to lower stability of DCJTB molecules, or (ii) the luminescence yield of the sensor layer suffers more severely than the bulk of the emitting layer due to a higher local concentration of hole space charges owing to its closer proximity to the HBL. To verify which of the above two mechanisms is behind the observed behaviour, similar EL spectral measurements are carried out on device I. Should the first mechanism be more dominant, we would expect to still observe faster degradation in DCJTB luminescence versus $Ir(ppy)_3$ luminescence , similar to that in case of device J, especially that the absence of the HBL leads to an increased electron-hole recombination in the sensor layer (figures 6.3).

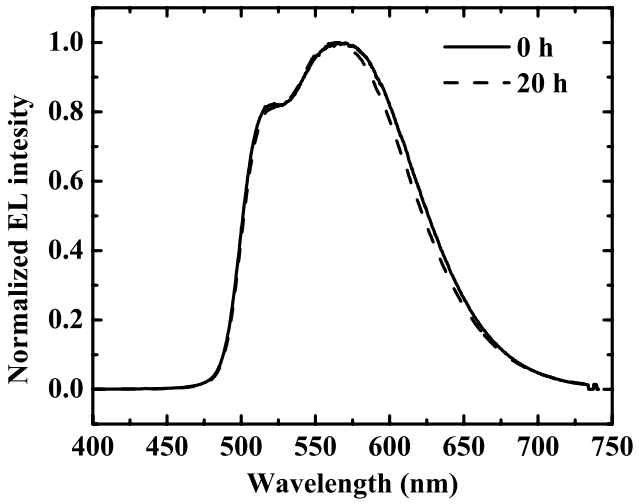

Figure 6.8 EL spectra of device I measured after aging for 0 and 20 hours at a constant current density of 20 mA/cm2.

Figure 6.8 shows the EL spectra from device I collected before and after aging. Clearly, in this case, aging brings about no significant change in EL spectra, ruling out this mechanism. This result confirms that the fast degradation of the sensor layer in device J must be induced by the higher concentration of space charges inside the sensor layer. Therefore, we can conclude that the use of a HBL in a PHOLED results in a higher concentration of space charges in the emitting layer, particularly near the HBL interface, and causes the faster degradation of luminescence from the sensor layer versus that from $Ir(ppy)_3$ in the emitter layer bulk. As different HBL materials can be expected to have different hole-blockage capacities, we can expect that they can diversely affect device stability. Preliminary results from a comparative study on different HBL materials, that is still underway, suggest that this may indeed be the case. The results from that study will be published elsewhere. At this moment, the underlying phenomena by which the space charges lead to increased quenching of excitons, hence the degradation of luminescence from the emitting layer are still unclear. It is possible that the high concentration of holes in the emitting layer leads to increased exciton quenching by means of

bimolecular hole-exciton annihilation processes, or that the trapped holes act as non-radiative hole-electron recombination centers [23,41,102,103]. A close examination of the effect of the magnitude of the reverse bias pulse on delayed EL characteristics shows that despite the increase in spike height after aging, the spike width, which reflects the release rate of trapped charge by the reverse bias, does not show any detectable change in "aged" versus "fresh" devices when a reverse bias of -10V is used. This can be seen from the normalized delayed EL characteristics in figure 6.9. A small increase in spike width can however be observed in the aged devices when using a reverse bias of only -5V, indicating that the release of trapped charges by the lower fields becomes more difficult with device aging, suggesting that the charges become more strongly trapped with aging, which, in turn, suggests an increase in deep hole traps with aging. This effect is more pronounced in case of the device with the HBL (figure 6.9b) where aging brings about a larger increase in spike width (at -5V) versus that in case of the device without the HBL (figure 6.9a). These results indicate that prolonged electrical driving of a PHOLED leads to an increase in the concentration of deep charge traps (and deeply trapped charges), and that the effect is intensified by the accumulation of hole space charges, evident in its more pronounced occurrence in the devices with the HBL. These observations support the notion that the loss of luminescence yield of the emitter, hence the loss of electroluminescence efficiency of PHOLEDs, is due to a gradual increase in deep traps (and deeply trapped charges) with electrical driving, that facilitate exciton quenching.

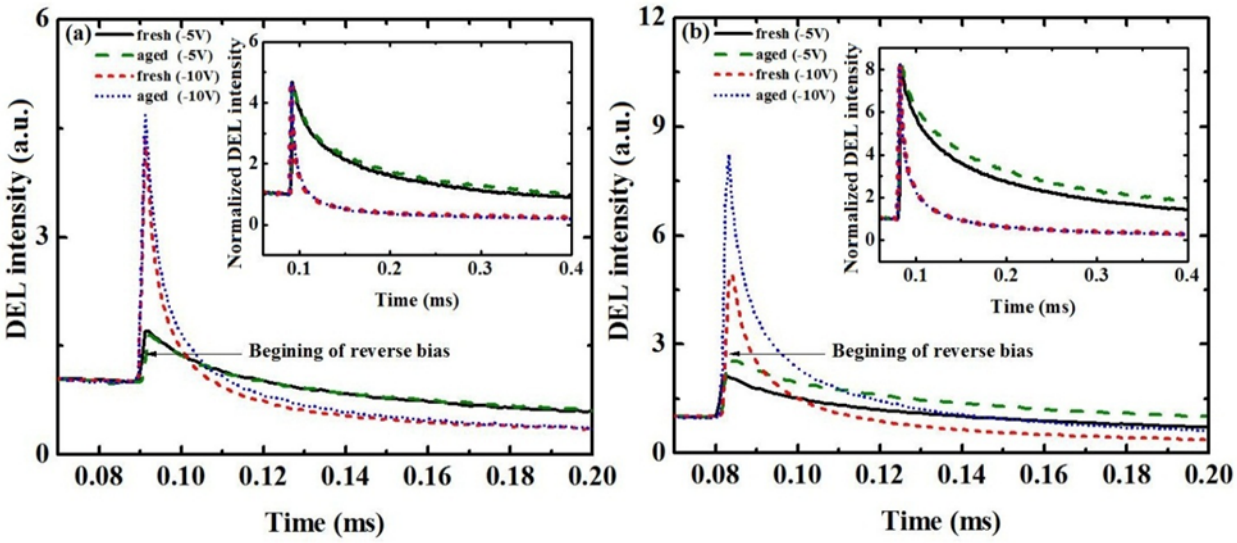

Figure 6.9 Intensity of delayed EL versus time in devices of structure (a)ITO/NPB (50 nm)/CBP:Ir(ppy)3 (40 nm)/Alq3 (30nm)/Mg:Ag, and (b) ITO/NPB (50 nm)/CBP:Ir(ppy)3 (40 nm)/BCP (10 nm)/Alq3 (30 nm)/Mg:Ag, collected before (fresh) and after aging (aged) for 20 hours at 20 mA/cm2. A 0.5 ms reverse bias pulse of magnitude -5V or -10V is applied during the data collection (pulse start point is as denoted by the arrows) The inset shows the same data, normalized to the maximum intensity.

6.3 Summary

In summary, two distinctive degradation mechanisms are observed in PHOLEDs, depending on whether the device contains a HBL or not. For a device without a hole blocking layer (HBL), excess holes penetrate into the electron transport layer (ETL), and lead to the deterioration of the ETL adjacent to the interface of the emitting layer. The lower electron transport capacity of the degraded ETL alters the balance in hole/electron injection into the emitting layer, and results in a decrease in the luminescence efficiency of the PHOLEDs. For a device with a HBL, on the other hand, holes accumulate and become trapped in the emitting layer, and result in a decrease in the luminescence efficiency of the PHOLEDs, likely due to their role in acting as exciton quenchers or as non-radiative charge recombination centers.

Chapter Seven: The Influence of the Hole Blocking Layers on the Electroluminescence Stability of Phosphorescent Organic Light Emitting Devices

In the previous chapter, it was shown that charge accumulation at the EML/HBL can effectively reduce the device EL intensity due to the TPQ process. In this chapter, devices with different HBLs with various extents of hole blocking capacities will be studied. It will be shown that there is a direct correlation between the hole blocking capacity of the HBL and EL degradation. This work has been published in Org. Electron., 12*,* **12***,* 2056-2060*,* 2011. *It has been reproduced with permission from the publisher under the license number 3212910492553.*

7.1 Introduction:

In order to increase PHOLED efficiency, it is customary to use means to confine charges and excitons inside the emission layer[63,71,104]. The large difference between the mobility of holes and electrons in organic semiconductor materials can cause a large fraction of carriers injected into the EML to leak to the other layers of the devices without recombining with counter carriers. To remedy this effect, blocking layers that help confine carriers (and excitons) into the EML, thereby increase efficiency, are widely used [93]. Despite their benefit to device efficiency, the effect of using these blocking layers on operational stability of PHOLEDs is not fully understood. For example, Scholz et. Al. [40] studied the chemical degradation of iridium(III)bis(2-methyldibenzo-[f,h]quinoxaline)(acetylacetonate) ($Ir(MDQ)_2acac$) phosphorescent red emitter in devices utilizing various hole blocking layers. Using laser desorption/ionization time-of-flight mass spectrometry (LDI-TOF-MS) technique, they found that Ir species at the EML/HBL interface can react with adjacent HBL material, suggesting it may cause EL degradation. The higher reactivity of 4,7-diphenyl-1,10-phenanthroline (BPhen)

and TPBi has therefore been concluded to be the main reason behind the generally lower EL stability of devices utilizing these two materials, versus, for example, BAlq, as HBLs. However, the correlation between the hole blocking capacities of these materials and device EL stability has not been addressed. Our recent studies show that the accumulation of holes in the EML plays a major role in the gradual loss in PHOLED efficiency [91]. It therefore becomes important to investigate and understand the role that HBLs play in that context. For example it is possible that devices with very high concentration of excitons and charges inside the EMLs may suffer faster degradation condition due to bimolecular phenomena such as exciton-charge quenching process [23,41].

7.2 Result and discussion:

Figure 7.1 shows changes in EL intensity with driving time in devices of the following structures:

ITO/NPB (50nm)/CBP:Ir(ppy)$_3$ (92%:8%, 40nm)/Alq$_3$ (30nm)/Mg:Ag/Ag (9:1, 100nm), (Named as No HBL).

ITO/NPB (50nm)/CBP:Ir(ppy)$_3$ (92%:8%, 40nm)/BAlq (10nm) /Alq$_3$ (30nm)/Mg:Ag/Ag (9:1, 100nm), (Named as BAlq HBL).

ITO/NPB(50nm)/CBP:Ir(ppy)$_3$ (92%:8%, 40nm)/BCP(10nm)/Alq$_3$ (30nm)/Mg:Ag/Ag (9:1, 100nm), (Named as BCP HBL).

All devices are driven using an AC driving scheme at an average current density of 20 mA/cm^2. The initial luminance and driving voltage of these devices are as shown in table 7.1. As

can be seen from the figure, the device with BCP HBL shows a significantly lower EL stability compared to the other two devices. The other two devices, on the other hand, show similar EL stability trends. We also measured the EL stability, also using AC driving, at the same initial luminance of 2000 cd/m^2. The results are shown in the inset of figure 7.1. Clearly in both aging schemes, the device with the BCP HBL shows much lower EL stability, whereas the devices with BAlq HBL and no HBL demonstrate the similar EL stability trends. We note that the observed stability is similar to that reported by some groups for the same device structure [94,95] but lower in comparison to other reports [96]. The wide variation in stability can be attributed to variations in ITO and organic materials obtained from different suppliers. In our case, the materials are purchased from the Luminescence Technology and are used as received.

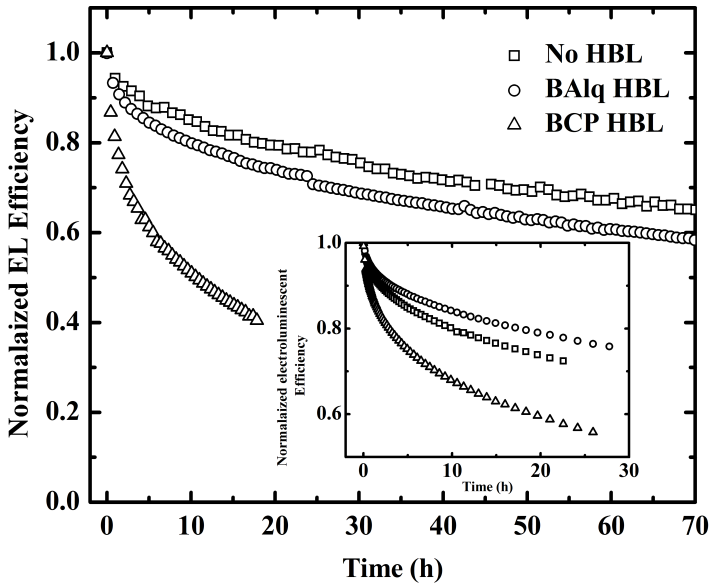

Figure 7.1 Normalized EL efficiency versus time of devices without HBL and with BAlq and BCP HBLs, under AC driving at an average current density of 20 mA/cm^2. Inset: Normalized EL efficiency versus time of an identical set of devices also driven using AC driving at an initial luminance of 2000 cd/m^2.

Table 7.1 Electrical and optical characteristics of the devices at 20 mA/cm^2 current density.

Device	Voltage(V)	Brightness(cd/m^2)	CIE
No HBL	10.4	1790	0.330, 0.597
BAlq HBL	10.58	2850	0.337, 0.597
BCP HBL	10.87	4130	0.331, 0.602

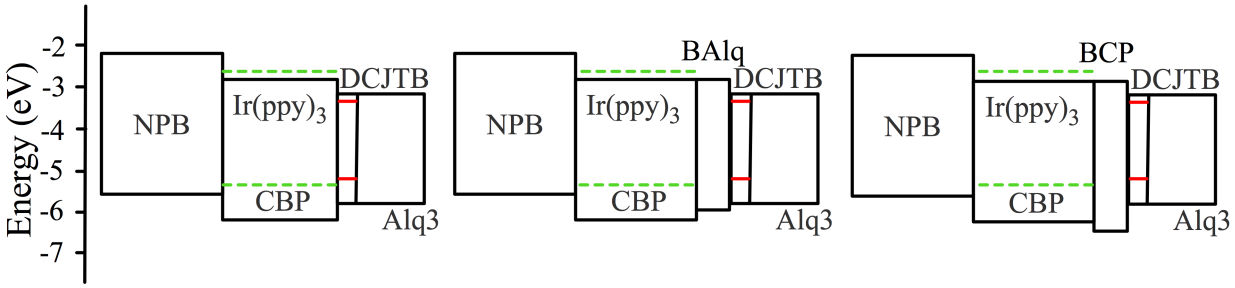

Figure 7.2 Schematic structure of devices A, B and C. Layer thicknesses used for these devices are as follow: NPB = 40 nm, CBP:Ir(ppy)$_3$ = 40 nm, Alq$_3$ = 25 nm, Alq$_3$:DCJTB = 5 nm, BAlq = 10 nm, and BCP = 10 nm.

To investigate the extent by which the HBLs reduce the leakage of holes from the EML towards the cathode, and any possible correlations with the observed changes in device stability when a HBL is used, we study a series of similar devices that contain a DCJTB-doped zone in the ETL, to act as a sensor layer. Figure 7.2 shows a schematic energy band diagram of these devices, whereas table 7.2 gives the driving voltage and EL intensity at 20 mA/cm^2 current density. Clearly the driving voltage of these devices is very similar to those without the sensor layer (<0.5 V) demonstrating that the presence of the sensor layer does not significantly modify charge injection and transport in the devices. We also measured the EL stability of these devices and found to be very similar to ones without sensor layer.

Table 7.2 Electrical and optical characteristics of the devices at 20 mA/cm^2 current density.

Device	Voltage(V)	Brightness(cd/m^2)	CIE
K	10.8	1640	0.371, 0.576
L	10.6	3200	0.345, 0.601
M	10.9	4660	0.336, 0.605

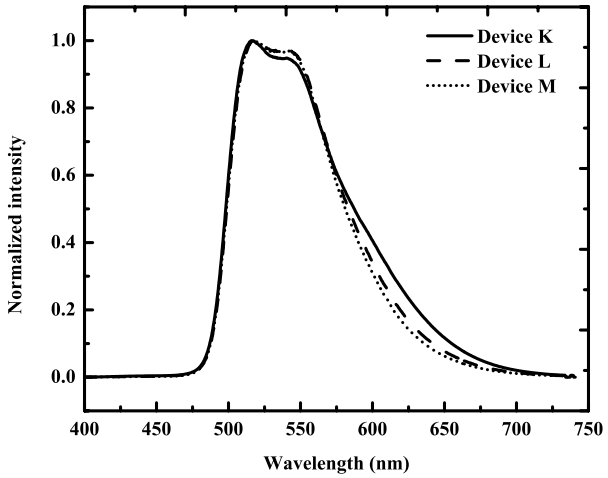

Figure 7.3 . Prompt EL spectra of devices K, L and M.

Figure 7.3 shows EL spectra collected from the same devices. As expected, all devices show strong emission bands in the green range, with the characteristic $Ir(ppy)_3$ peak at 511nm. The spectrum of device K is slightly broader in the red range, suggestive of some red emission from DCJTB sensor layer as would be expected due to the absence of HBL. To gain more insights about differences among these devices, we study the devices using delayed EL measurements. Figure 7.4 shows delayed EL spectra of devices K, L and M. As can be seen from the figure, delayed EL spectra show much more pronounced emission from DCJTB (611nm peak band) in

case of devices K (no HBL) and L (BALq HBL), but not in case of device M (BCP HBL) revealing that, unlike BCP, hole blockage by BAlq is only partial. The fact that emission from the DCJTB sensor layer is much more pronounced in delayed EL (i.e. figure 7.4) versus prompt EL (i.e. figure 7.3) can be attributed to the fact that holes are much less mobile in Alq_3 (due to its very low hole mobility) and therefore get essentially trapped on reaching the ETL. As residual electrons get swept back from the EML and HBL towards the cathode by the reverse bias pulse, they recombine with these trapped holes producing the observed delayed EL from the sensor layer. Regardless of the exact mechanism, the results in figure 7.4 convincingly prove that more holes reach the ETL in case of device L (BAlq HBL) than in case of device M (BCP HBL).

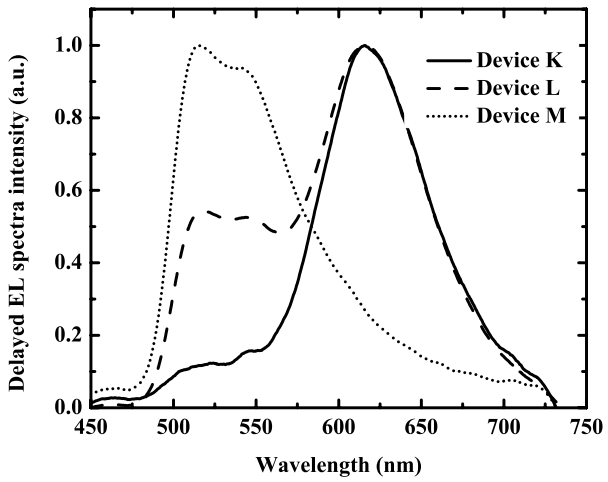

Figure 7.4 Delayed EL spectra of devices K, L and M.

Finding that the use of a marginally blocking HBL (i.e. BAlq) results in a marginal decrease in device EL stability (from figure 7.1), whereas the use of a strongly blocking HBL (i.e. BCP) results in a significant decrease in EL stability, the question whether the observed changes in EL stability in figure 7.1 are due to variations in the extent of accumulation of holes in the EML naturally arises. To determine the relative concentration of trapped charges in the EML of these devices, we measure changes in their delayed EL intensity with time, monitoring the effect of the reverse bias pulse. For these measurements, devices without the sensor layer, (and therefore identical to the ones used in EL stability measurements of figure 7.1) are used in order to ensure that all delayed EL originates from the EML. Figures 7.5a, 7.5b and 7.5c show the delayed EL signal versus time elapsed from the end of the forward bias pulse obtained from the devices without HBL, with BAlq HBL and with BCP HBL, respectively; collected before and again after 20 hours of electrical aging at 20 mA/cm^2 current density in each case (denoted by "fresh" and "aged" on the figures in each case).

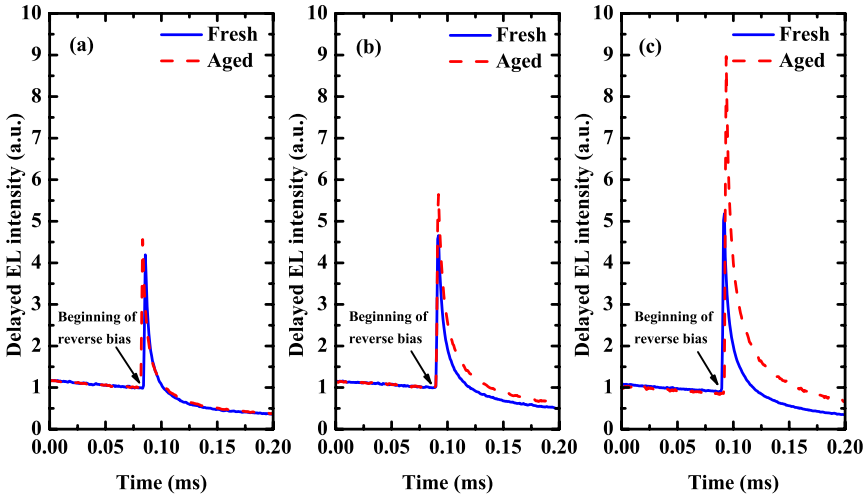

Figure 7.5 Delayed EL intensity of devices a) without HBL, b) with BAlq HBL and c) with BCP HBL, collected before (Fresh) and after aging (Aged) for 20 hours at 20 mA/cm^2 current density.

As can be seen from the figures, the application of the reverse bias causes a sudden increase in delayed EL intensity, which appears as a spike. The appearance of spike is an indication of a sudden release of trapped charges, which then recombine producing electroluminescence. A comparison of the spike heights in the fresh devices correlate with the expected variation in the extent of a hole space charge build-up in the EML among the three devices, with the device without the HBL showing the smallest spike (hence the smallest space charge), whereas the device with the strongly blocking HBL (i.e. BCP) demonstrating the highest spike (hence the largest space charge). Furthermore, a comparison of the spike heights due to aging reveals that the device without the HBL demonstrates the smallest increase, whereas the device with the strongly blocking HBL (i.e. BCP) demonstrates the largest increase, indicating the largest increase in the number of trapped charges in the EML upon prolonged electrical driving in the latter. The results therefore show a strong correlation between the accumulation of holes in the EML and the loss in EL efficiency of the PHOLEDs. In this regard, the efficiency loss may be due to increased exciton-polaron annihilation, which, as a bimolecular interaction, will increase with the concentration of holes trapped in the EML. The increase in trapped charges with electrical aging suggests that the effect may also be associated with an increase in concentration of deep charge traps, which can act as non-radiative recombination centers, and hence also contribute to the loss in device efficiency.

To that end, device stability is strongly influenced by the use of a HBL, where the use of a strongly blocking material (e.g. BCP) will significantly increase the build-up of holes in the EML, and hence accelerate the EL degradation of the device.

7.3 Summary

In summary, delayed EL measurements are used to investigate electroluminescence stability in PHOLEDs containing typical HBLs. The results show a strong correlation between the extent of hole blockage capacity of the HBL and the deterioration in device EL efficiency, pointing to the major role that the build-up of hole space charges in the emitting layer plays in EL degradation. In this regard, the use of a strongly blocking material (e.g. BCP) significantly increases the build-up of holes in the EML, and accelerates EL degradation.

Chapter Eight: Causes of Driving Voltage Rise in Phosphorescent Organic Light Emitting Devices during Prolonged Electrical Driving

In this chapter, the causes behind the voltage rise during device operation will be investigated. It will be shown that voltage rise is associated with the formation space charge at the EML/HBL interface. It will also be shown that, during device operation, TTA and concentration of host excitons gradually decrease due to the increase of trapped charges. In addition, a method to reduce voltage rise will be presented. This work has been published in J. Appl. Phys. Lett., 17*,* **101***,* 173502, 2012*. It has been reproduced with permission from the publisher under the license number 3212910072492.*

8.1 Introduction

In general, the electrical stability of any OLED has two aspects: i) the stability of its electroluminescence efficiency (simply referred to as the electroluminescence stability) and ii) the stability of its driving voltage. The first relates to the gradual decrease in device quantum efficiency with driving time under constant current driving, whereas the latter relates to the increase in driving voltage required to maintain the driving current.

Several factors have been identified as possible root causes for the limited electroluminescence stability in OLEDs in general. Example of these factors include: the instability of organic molecules in certain charged states[19,105]; the presence of fixed positive space charges [105]; the diffusion of mobile ionic impurities [106]; the leakage of charge carriers and excitons [93]; and various bimolecular interactions such as TTA and TPQ [23,41]. Contrary to electroluminescence stability, the root causes behind the increase in OLED driving voltage during prolonged electrical driving have not been deliberately investigated, and remain essentially unknown, especially for PHOLEDs. A report by Kondakov suggested that the

accumulation of positive space charges at the HTL/ETL interface plays a role in voltage rise in bilayer fluorescent OLEDs. However, the causes of voltage rise in typical PHOLEDs, which, in comparison to fluorescent OLEDs, generally utilize different materials and contain more layers, remain essentially unknown. The driving voltage stability is, on the other hand, an important issue, especially for active matrix display panels in which each pixel is driven by its own integrated circuit. Since the circuits are typically designed to provide a certain power output, a significant change in the voltage required to drive an OLED creates challenges for driving circuits.

8.2 Result and discussion

In previous chapter it was found that the accumulation of holes inside the EML accelerates electroluminescence degradation of PHOLEDs. It was shown that increasing the confinement of holes inside the EML, for example, by means of using a HBL, accelerates the decrease in EL efficiency. The deterioration in EL efficiency was also found to be associated with a decrease in the photoluminescence quantum yield of the EML, likely due to an increase in triplet-polaron quenching. In order to investigate if the same phenomenon also plays a role in the gradual increase in device driving voltage during prolonged electrical driving, we conduct a comparative study on PHOLEDs containing HBLs (BAlq or BCP) or no HBL. The devices have the following structures:

ITO/MoO_3(10nm)/NPB(40nm)/CBP:$Ir(ppy)_3$ (8%) (40nm)/Alq_3 (30nm)/Mg:Ag

ITO/MoO_3(10nm)/NPB(40nm)/CBP:$Ir(ppy)_3$ (8%) (40nm)/BAlq(10nm)/Alq_3 (30nm)/Mg:Ag

ITO/MoO_3(10nm)/NPB(40nm)/CBP:$Ir(ppy)_3$ (8%) (40nm)/BCP(10nm)/Alq_3 (30nm)/ Mg:Ag

Figure 8.1 shows typical change trends in device driving voltage required to maintain a constant current density of 20 mA/cm^2, represented as ΔV, where ΔV = the driving voltage V (at any time t) – V (at t=0) . At this current density, the initial driving voltages of the devices without HBL, with BAlq HBL and with BCP HBL are 12.8 V, 13.4 V and 14.2 V, respectively. The differences in initial voltage can be attributed to the various hole blocking capacities of the devices. In case of the device without HBL, holes can easily drift from the EML into the adjacent electron transport layer since CBP/Alq_3 interface does not block holes. On the other hand, in devices with BAlq and BCP HBLs, holes are confined inside the emission layer by the hole blocking barrier at the EML/HBL interface which arises from the deeper HOMO of the HBL material in comparison to that of the EML. This barrier is lower in case of BAlq HBL, causing the hole blockage to be only partial [88]. As can be seen from figure 8.1, the voltage rise trends are different among the devices, and correlate with the extent of hole confinement in the EML, where the device with the strongest hole confinement in the EML (i.e. with BCP HBL) displays the fastest rise in voltage whereas the device with the least hole confinement (i.e. with no HBL) displays the slowest rise. The results suggest that the ΔV trends depend on the concentration of accumulated holes at the EML/HBL interface.

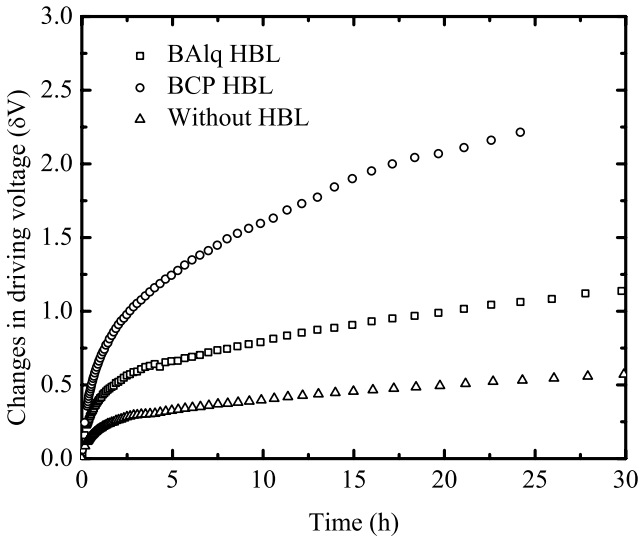

Figure 8.1 Changes in driving voltage of typical PHOLEDs without and with BAlq and BCP hole blocking layers under the applied 20 mA/cm^2 current density.

In order to verify this and further understand the possible role of holes in the voltage rise, we fabricate and test a series of devices, which include a neat CBP, of various thicknesses, next to the EML/HBL interface. In these devices, the thickness of the $Ir(ppy)_3$ -doped layer is adjusted so as to keep the total device thickness the same. The general device structure is: ITO/MoO3 (10 nm)/ NPB (40 nm)/ CBP:Ir(ppy)3 (40-x nm)/ CBP (x nm)/BAlq (10 nm)/Alq3 (30 nm)/Mg:Ag, where x represents the thickness of the neat CBP layer. The electroluminescence characteristics of these devices are summarized in Table 8.1. As can be seen from the table, all devices exhibit comparable EL levels despite of differences in the thickness of the $Ir(ppy)_3$ -doped layer. This shows that the electron-hole (e-h) recombination zone is located in the EML region close to the HTL, which agrees well with previous reports [92,107].

Table 8.1 Electroluminescence characteristics of the devices with different thicknesses of neat CBP layer at the EML/HBL interface.

CBP(x nm)	Voltage(V)	Brightness(cd/m^2)	CIE
3	12.29	3870	0.331, 0.596
5	12.63	3880	0.329, 0.597
0	13.3	3810	0.328, 0.603

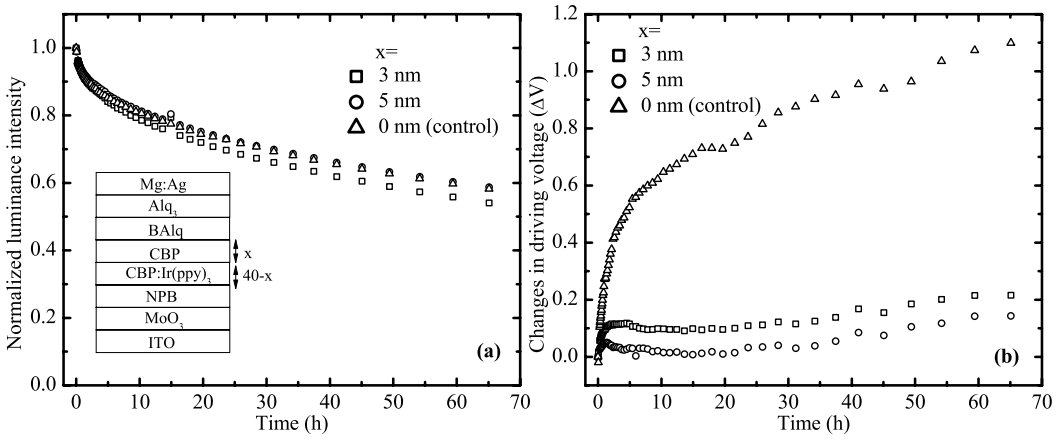

Figure 8.2 a) Normalized luminance intensity and b) changes in driving voltage of devices with and without CBP spacer layer at the EML/HBL interface under electrical aging at 20 mA/cm^2 current density. The inset shows a schematic diagram of the device structure.

Figures 8.2a and 8.2b show the luminance intensity and operating voltage of these devices versus time of driving at 20mA/cm^2 current density, respectively. As can be seen from figure 8.2a, all devices show comparable EL stability trends, indicating that changing the EML/HBL interface by means of introducing a neat CBP layer does not significantly affect device EL stability suggesting EL stability is not primarily governed by phenomena at this interface. Conversely, and quite interestingly, the presence of a neat CBP layer affects the voltage rise trends quite significantly (Figure 8.2b). For instance the control device (device without a CBP

layer) shows a voltage rise of about 1 V after 70 hours of operation whereas the voltage rise in the device with the 3 nm neat CBP layer is only about 0.1 V over the same period of time. Clearly, this observation suggests that the two device stability aspects (i.e. EL stability and driving voltage stability) are not always coupled.

In order to understand why the use of a neat CBP layer at the EML/HBL can reduce the voltage rise rate, one has to look at the charge transport and recombination mechanism in the EML. In general, due to the large energy barrier for hole injection from NPB to CBP, holes are injected from the NPB layer into the EML mostly onto $Ir(ppy)_3$ sites directly[33,90]. Subsequent to injection, holes are transported into the EML by hopping on both $Ir(ppy)_3$ sites and (but to a much less extent) on CBP sites [90]. On the other hand, due to the very small energy difference between CBP and BAlq LUMO levels (2.8 eV and 2.9 eV, respectively), electrons are mostly injected and transported onto CBP sites [108]. This is also evident from the initial driving voltage and brightness levels of devices containing the neat CBP layer, where the absence of $Ir(ppy)_3$ from the region adjacent to the HBL interface does not result in an increase in the initial driving voltage or a decrease in the luminance, as would be expected should $Ir(ppy)_3$ be assisting electron injection and/or transport in the EML. As holes mostly reside on $Ir(ppy)_3$ sites whereas electrons are transported efficiently by CBP sites, some holes on $Ir(ppy)_3$ sites at the HBL interface can stay without recombination. One would expect that the number of such "un-recombined" holes near the EML/HBL interface to increase during device operation. Therefore, in order to offset the effect of these trapped positive charges at the EML/HBL interface and maintain the electric field inside the EML that is required to sustain the same current, the positive potential applied on the anode with respect to the cathode must increase, hence the increase in driving voltage. As in case of the devices with the neat CBP layer $Ir(ppy)_3$ is absent

from the region near the HBL, the number of trapped holes near the HBL is significantly lower, hence the much smaller voltage rise.

In order to see if removing $Ir(ppy)_3$ from the EML in the vicinity of the HTL/EML interface may similarly affect the driving voltage rise, we fabricate and test another series of devices that contain a neat CBP layer at the HTL/ EML interface. The general device structure is: ITO/MoO3 (10 nm)/ NPB (40 nm)/ CBP (x nm)/ CBP:$Ir(ppy)_3$ (40-x nm)/BAlq (10 nm)/Alq3 (30 nm)/Mg:Ag. Table 8.2 summarizes the electroluminescence characteristics of these devices whereas Figure 8.3 shows the increase in driving voltage (presented as ΔV) during continuous electrical driving at 20 mA/cm^2. As can be seen from the table, introducing a thin neat CBP layer at (i.e. removing $Ir(ppy)_3$ from) the region near the HTL/EML interface results in a significant reduction in brightness. This indicates that the majority of e-h recombination occurs close to the HTL, in agreement with previous reports[92].

Table 8.2 Electroluminescence characteristics of the devices with different thicknesses of neat CBP layer at the HTL/EML interface.

CBP(x nm)	Voltage(V)	Brightness(cd/m^2)	CIE
3	12.12	2950	0.358, 0.583
5	13.14	2180	0.343, 0.567
0	13.02	3330	0.351, 0.589

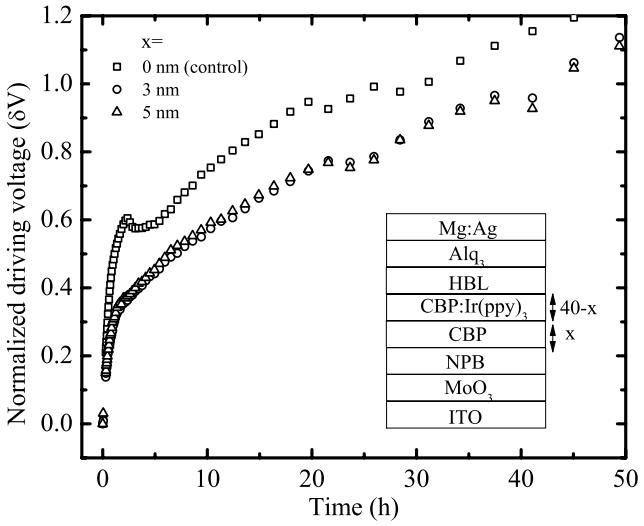

Figure 8.3 Changes in driving voltage of devices with and without neat CBP layer at the HTL/EML interface under electrical aging at 20 mA/cm^2 current density. The inset shows a schematic diagram of the device structure.

Furthermore, as figure 8.3 shows, the devices show similar voltage rise trends indicating that the gradual increase in driving voltage with electrical driving is not strongly influenced by removing $Ir(ppy)_3$ from the EML near the HTL/EML interface. This is not surprising considering that the e-h recombination zone is located close to the HTL, and therefore the concentration of any holes that may remain without recombination "permanently" on $Ir(ppy)_3$ sites at this region of the EML can be expected to be small. As such, removing hole trap sites (such as by removing $Ir(ppy)_3$, which generally acts as a hole trap in CBP [92,99]) will not have a major effect on the long term voltage rise trend of the PHOLED.

Finding that removing $Ir(ppy)_3$ from the EML region adjacent to the EML/HBL interface leads to a significant improvement in PHOLED driving voltage stability , likely due to a reduction in the concentration of hole trap sites, and, consequently the concentration of trapped holes, one would expect that introducing e-h recombination centers in the same region to have a similar effect. In this case, the presence of recombination centers would increase e-h

recombination in this region, hence would result in a reduction in build-up of residual holes. To investigate this effect, we fabricate and test devices in which a narrow band-gap material is doped into the EML, in addition to the $Ir(ppy)_3$, near the EML/HBL interface. For this purpose, we use Platinum Octaethyl Porphine (PtOEP) as a narrow band gap material (The band gap of PtOEP and $Ir(ppy)_3$ is 2.5 eV and 3.3 eV, respectively [30]). The general device structure is: ITO/MoO_3 (10nm)/NPB (40nm)/CBP:$Ir(ppy)_3$ (8%) (35nm)/CBP:$Ir(ppy)_3$:PtOEP (x%) (5nm)/BAlq (10nm)/Alq_3 (30nm)/Mg:Ag. The electroluminescence characteristics of a series of devices with different concentrations of PtOEP are summarized in Table 8.3. Figure 8.4 shows the driving voltage (presented as ΔV) during continuous electrical driving at 20 mA/cm^2. As can be seen from the figure, introducing the PtOEP slows down the increase in driving voltage. To understand the role PtOEP in reducing the voltage rise, we compare the electroluminescence (EL) spectra of the device containing 10% PtOEP at different bias voltages, as shown in figure 8.5. As can be seen from the figure, two emission peaks at 510 nm and 650 nm, corresponding to emission from $Ir(ppy)_3$ and PtOEP respectively, are observed. The relative intensity of the two peaks varies with the bias voltage. The $Ir(ppy)_3$ emission peak is higher than the PtOEP peak at high voltages (i.e. at voltage >9V) but is lower at lower voltages (< 9V) , and becomes essentially undetectable at voltages below $\leq$ 6 V. This suggests that the recombination zone is mostly located near the EML/HBL interface at low bias voltages but gradually shifts towards the HTL as the voltage is increased. Observing emission from PtOEP at low driving voltages suggests that hole injection and transport in the EML occurs quite easily. As the voltage is increased, electron injection and transport into the EML becomes increasingly easier, leading to the gradual shift in the e-h recombination zone towards the HTL. The fact that PtOEP emission can be observed at all voltages indicates that PtOEP sites act as efficient e-h recombination

centers, owing to the material's ability to trap both holes and electrons in a CBP:$Ir(ppy)_3$ system. Its effectiveness in trapping electrons is evident from its ability to partially pin the e-h recombination zone to the region near the HBL interface. It is also evident from the data in Table 8.3, which shows that increasing PtOEP concentration leads to an increase in the initial driving voltage of a device, consistent with an electron trapping effect. In acting as efficient e-h recombination centers, PtOEP sites expectedly facilitate the "consumption" of holes through recombination, causing the concentration of residual holes in the EML near the HBL interface to be reduced. The improvement in driving voltage stability observed on introducing the PtOEP (figure 8.4) therefore further proves that the accumulation of holes near this interface is the main factor behind the increase in driving voltage during PHOLED operation.

Table 8.3 Electroluminescence of the devices with different PtOEP concentrations at 20 mA/cm^2 current density.

PtOEP concentration (%)	Voltage(V)	Brightness(cd/m^2)	CIE
1	11.8	2470	0.346, 0.590
2	11.62	2000	0.349, 0.587
5	12.14	1580	0.356, 0.579
10	12.31	1670	0.353, 0.581
0	11.41	3600	0.327, 0.599

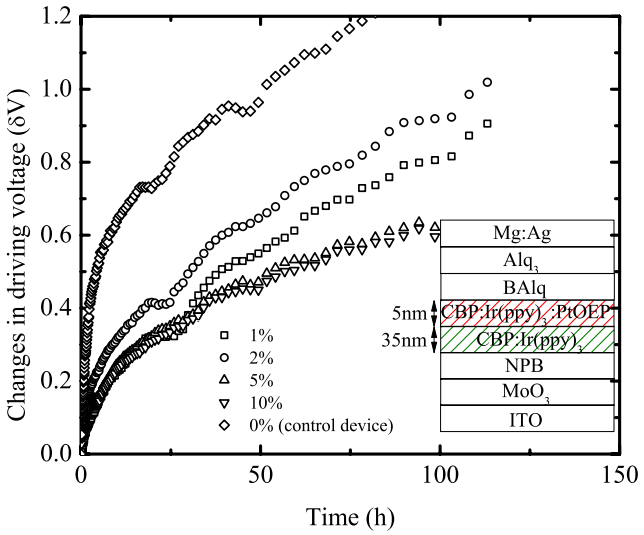

Figure 8.4 Changes in driving voltage of devices with various PtOEP concentrations aged at 20 mA/cm^2 current density. The inset shows a schematic diagram of the device structure.

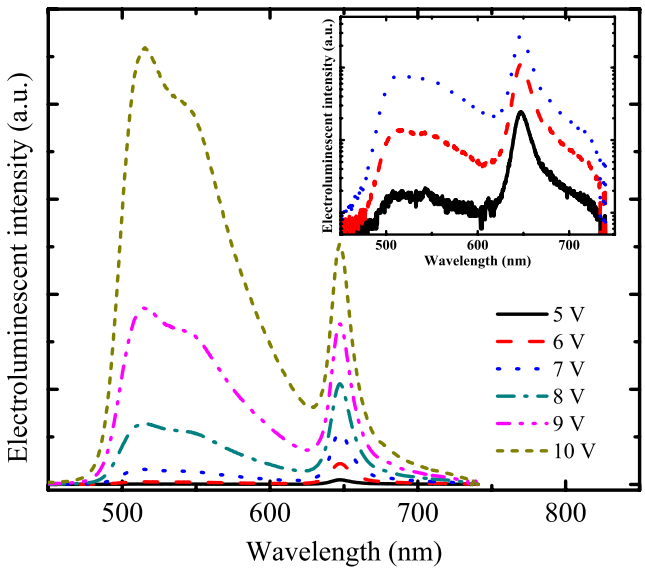

Figure 8.5 Electroluminescent intensity of the device with 10% PtOEP doped at 5 nm region adjacent to the HBL interface under various forward voltages. The inset shows the magnified EL spectra at 5, 6 and 7 volts forward voltages.

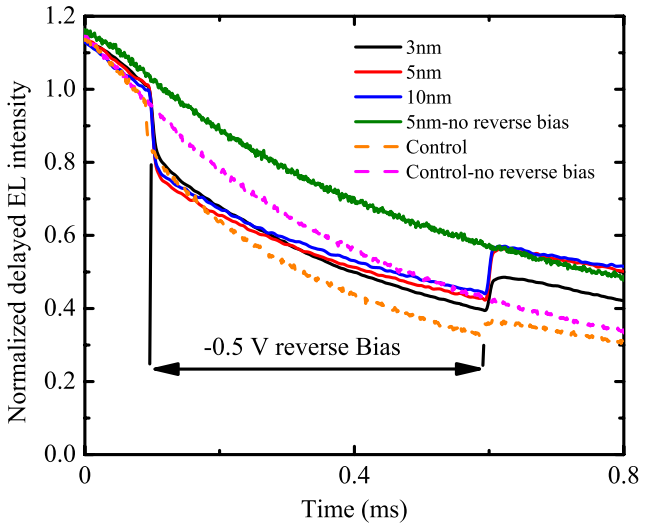

Figure 8.6 Delayed EL intensities of the devices with different thicknesses of neat CBP layer under -0.5 V reverse bias.

In order to obtain more insights about the role of the neat CBP layer at the EML/HBL interface in improving driving voltage stability of the devices, we use delayed EL measurements to study devices with and without such layers. Figure 8.6 displays the delayed EL signal versus time elapsed from the end of the forward bias pulse collected from devices containing a neat CBP layer (3, 5 or 10 nm thick) at the EML/HBL interface and also from a control device that does not contain a neat CBP layer(device structure: ITO/MoO3 (10 nm)/ NPB (40 nm)/ CBP:Ir($ppy_{)3}$ (40-x nm)/ CBP (x nm)/BAlq (10 nm)/Alq_3 (30 nm)/Mg:Ag, where x represents the thickness of the neat CBP layer). Time 0 on the x-axis corresponds to 0.3 ms after the end of the forward bias pulse. It should be noted that spectral measurements show that the delayed EL corresponds to $Ir(ppy)_3$ emission. As can be seen from the figure, the delayed EL from all devices with a CBP layer exhibits a sudden decrease on the application of the reverse bias pulse, but rebounds, at least partially, at the end of the reverse bias pulse. This recovery is partial in

case of the device with the 3 nm CBP layer but is almost complete in case of the devices with the 5 and 10 nm CBP layers. (Note: delayed EL characteristics from a control device and from a device with 5 nm CBP layer that are not subjected to the reverse bias pulse, labelled "no reverse bias" is also shown on the same for comparison). In contrast, the control device (i.e. without a neat CBP layer) shows only a modest decrease in delayed EL at the beginning of the reverse bias pulse, and also a relatively much smaller recovery at the end of the pulse. As a recovery at the end of the reverse bias indicates that host-host TTA contributes significantly to the observed delayed EL[33], the results indicate that the concentration of host triplet excitons is higher in devices containing a neat CBP layer, and generally increases with the thickness of the layer. It follows therefore that these triplet excitons originate in the neat CBP layer. That this effect appears to saturate as the thicknesses of the layer exceeds 5 nm can be due to the fact that only triplet excitons in this neat layer that are within a distance from the CBP/ $Ir(ppy)_3$ layer interface equal to the Forster radius for energy transfer (typically ~ 5nm) are able to undergo efficient energy transfer to $Ir(ppy)_3$, and hence contribute to the delayed EL signal. Figure 8.7 shows delayed EL from the same devices measured before and again after 80 hours of continuous electrical driving at a current density of 20 mA/cm^2, denoted to by "fresh" and "aged", respectively. As can be seen from the figures, prolonged electrical driving affects the extent of recovery in delayed EL at the end of the reverse bias pulse, causing it to almost disappear in case of the control device (figure 8.7a), and to become clearly lower in the devices with the 3 nm and 5 nm CBP neat layers (figures 8.7b and 8.7c, respectively). On the other hand, the extent of recovery remains almost unchanged in case of the device with the thicker (i.e. 10 nm) CBP neat layer (figure 8.7d).

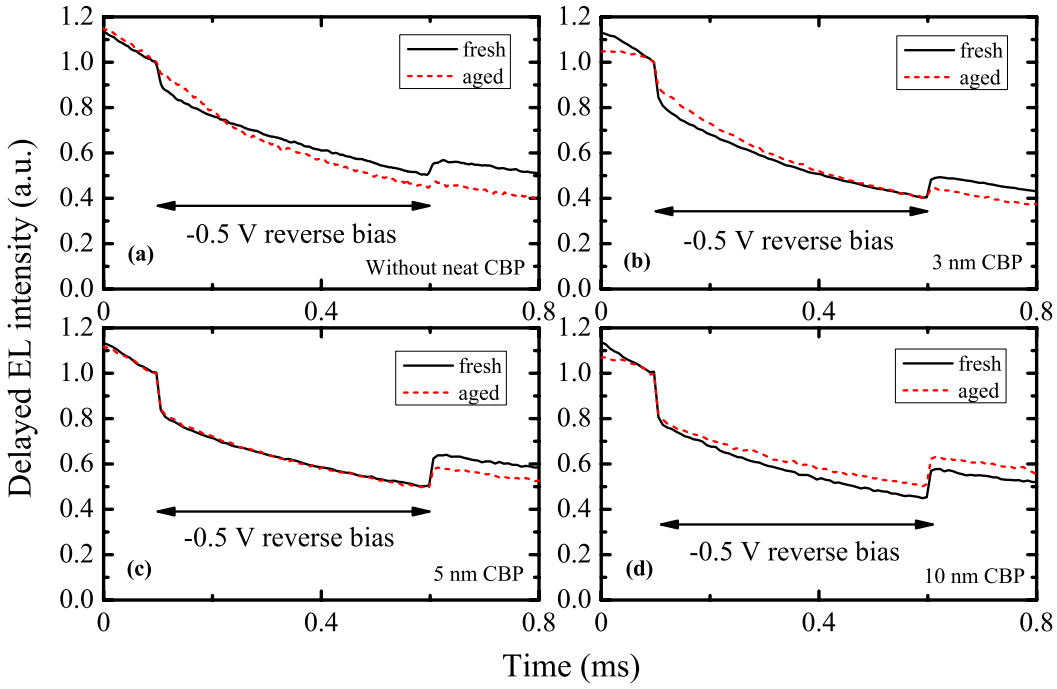

Figure 8.7 Delayed EL signal of devices a) without a neat CBP layer, with b) 3 nm CBP, c) 5 nm CBP and d) 10 nm CBP layer before and after 80 hours of electrical aging at 20 mA/cm^2 current density.

This reduction in recovery, which reflects a decrease in the underlying TTA process, points to a decrease in the concentration of CBP triplet excitons. The decrease in triplet exciton concentration suggests the increase in charge concentration with prolonged electrical driving, which results in an increased quenching of the triplet states due to triplet-polaron interactions [103]. The results therefore suggest that the use of a neat CBP layer of sufficient thickness (e.g. 10 nm) at the EML/HBL interface reduces the build-up of trapped charges in the vicinity of the interface during prolonged electrical driving, evident in the almost unchanged delayed EL characteristics observed in this case (figure 8.7d). That the concentration of these charges is higher in devices with a thinner neat CBP layer (and highest in the device with no neat CBP

layer) indicates that such charges may be trapped on $Ir(ppy)_3$ sites in the vicinity of the interface. As $Ir(ppy)_3$ transports holes mostly [108], such trapped charges would be expected to be holes. In this regard, removing $Ir(ppy)_3$ from the vicinity of the interface (i.e. by having a neat CBP layer) therefore eliminates trap sites, thereby preventing the build-up of this positive charge in the vicinity of the interface, hence the much higher driving voltage stability observed in figure 8.2b. It is also possible that the EML/HBL interface contains a high density of hole traps, perhaps due to increased structural defects near the interface. Removing $Ir(ppy)_3$ from this region eliminates the hole transport pathway, hence prevents the population of these interfacial traps with holes.

8.3 Summary

In conclusion, our studies show that the gradual increase in driving voltage often observed with prolonged electrical driving of PHOLEDs is mainly governed by the accumulation of holes at the EML/HBL interface. Results from delayed EL measurements suggest the build-up of a hole space charge in the vicinity of this interface with prolonged electrical driving, reducing the build-up of hole space charges in this region, for example, by means of eliminating guest molecules from the vicinity of the interface, leads to a significant improvement in the stability of PHOLED driving voltage.

Chapter Nine: Summary and Future works

9.1 Summary

In this thesis underlying mechanisms associated with the bimolecular interactions and their roles on the PHOLEDs efficiency roll-off and EL degradation are investigated. Various methods including delayed EL measurements are used to study the devices under the short-term and long-term operations.

It was found that efficiency loss due to TPQ is mainly caused by charges within the bulk of the EML rather than by charges at the HTL/EML interface. Charges on the guest rather than those on the host are found to be the most efficient in quenching excitons, revealing that guest polaronic species are the most detrimental to device efficiency. In addition, recombination of electrons and holes on the host material generally leads to higher device efficiency in comparison to cases where recombination occurs on the guest material. Although electron-hole recombination on the host tends to produce higher device efficiency, host e-h recombination is generally also associated with significant efficiency roll-off due to the quenching of the host triplet excitons primarily as a result of host-host TTA.

Furthermore, results from the study of devices with various guest concentrations reveal that as the concentration of the guest molecules increases and the creation of host triplet excitons subsides (since most e-h recombinations occur on the guest), host-host TTA decreases, hence the efficiency roll-off. In such cases, quenching is mostly caused by polarons residing on guest sites. At optimum guest concentrations (~8 % Vol.), a balance between host e-h recombination and guest e-h recombination is reached, and thus minimal TTA and TPQ.

Turning to the device operational stability, two distinctive degradation mechanisms are observed in PHOLEDs, depending on whether the device contains a HBL or not. For a device without a HBL, excess holes penetrate into the ETL and lead to the deterioration of the ETL adjacent to the interface of the emitting layer. The lower electron transport capacity of the degraded ETL alters the balance in hole/electron injection into the emitting layer, and results in a decrease in the luminescence efficiency of the PHOLEDs. For a device with a HBL, on the other hand, holes accumulate and become trapped in the emitting layer, and result in a decrease in the luminescence efficiency of the PHOLEDs due to their role in acting as exciton quenchers or as non-radiative charge recombination centers. Furthermore, the results show a strong correlation between the extent of hole blockage capacity of the HBL and the deterioration in device EL efficiency, pointing to the major role played by the build-up of hole space charges in the emitting layer in EL degradation. In this case, gradual increase of trapped charges in the EML enhances the TPQ process and hence exciton quenching manifests as a reduction of TTA. In addition, gradual increase in driving voltage often observed with prolonged electrical driving of PHOLEDs is mainly governed by the accumulation of holes at this interface. Reducing the build-up of hole space charges in this region, such as by eliminating guest molecules from the vicinity of the interface, leads to a significant improvement in the stability of PHOLED driving voltage.

9.2 Recommendations for future works

It was found that host-host TTA can considerably reduce the efficiency. Therefore, it is recommended to employ different approaches in order to effectively suppress this bimolecular interaction. In this matter, employing double doped EML with efficient energy transfer from the host to the dopants may reduce the efficiency roll-off. Besides, host material with short triplet

exciton lifetime may also decrease the host-host TTA. It is worthwhile exploring different host materials with various triplet exciton lifetimes in order to gain more insights about this type of TTA.

As presented in chapter five, presence of positive charges on the guest sites can significantly reduce the device efficiency. However, due to the nature of host:guest system studied in this work in which electron trapping by the guest molecules is insignificant, the possible role of trapped electrons on the efficiency roll-off is unclear. Therefore, it might be interesting to extend this investigation for different host:guest systems where guest molecules trap electrons. In this case, delayed EL and photoluminescence studies of several hole only and electron only devices are recommended in order to understand which type of charge carrier is more detrimental to the device efficiency.

Charge injection from the HTL into the EML is found to be the critical factor for improving the device efficiency. In case of devices where direct hole injection from the HTL into the host is efficient, devices demonstrate high efficiency. It is recommended to investigate devices with various hole injection barriers at the HTL/EML interface to further verify this observation. In addition, as demonstrated, direct hole injection from the HTL into the guest molecules reduces the device efficiency in contrast to some reported studies proposing that high efficiency can be achieved by direct injection of charge carriers into the guest molecules. One possible reason for this discrepancy is that in CBP:$Ir(ppy)_3$ host:guest system electrons can be easily injected from the ETL into CBP because of the small electron injection barrier at the CBP/ETL interface while hole injection from the HTL into $Ir(ppy)_3$ is more favourable, which in turn introduces charge imbalance in the EML and resulting severe TPQ. Therefore, it is recommended to explore and compare the possible different efficiency behaviours of devices in which direct electron injection

from the ETL into guest is more favourable as well as cases where direct electron injection from the ETL into the host is efficient. Moreover, studying devices in which both electron and hole injections occur directly into the guest molecules and into the host matrix is worthwhile.

Furthermore, for development of highly efficient PHOLED, it is recommended to employ a host:guest system in which charge trapping on the guest is minimal. For this interest, energy level alignment between charge transport layers and emission layer and employing host and guest materials with small difference between their energy bandgaps may enhance the efficiency.

Energy transfer from the host into the guest is an efficient process that leads to high efficiency in comparison to the e-h recombination on the guest. However, the reasons behind this observation are not fully known and require further investigation. One possible explanation is that the presence of charge carrier on the guest may efficiently quench the triplet guest exciton while quenching of host excitons by charges on the guest may not be as severe as guest TPQ.

In addition, it was found that hole space charge in the EML significantly reduces the device operational lifetime due to the TPQ by the trapped charges during long-term device operation. However, it is still not clear whether the formation of trapped sites is associated with the degradation of host molecules or due to the degradation of guest emitters. Nevertheless, it appears that during long-term device operation, host-host TTA reduces after the electrical aging; this suggests a decrease in the concentration of host triplet excitons possibly due to the degradation of host molecules. As TPQ accelerates the EL degradation, it is also worthwhile to explore whether charges on the guest lead to the fast EL decrease or charges on the host molecules.

Moreover, it was demonstrated that TPQ is more pronounced at the interfaces of the EML and charge transport layers. Interestingly, host-host TTA and concentration of triplet excitons away from the interfaces do not change after electrical aging; this suggests that degradation of devices in which charge accumulation at the interfaces is insignificant may not be due to the TPQ. Therefore, it is recommended to explore other factors that possibly limit the device operational stability.

References

[1] A. Bernanose, M. Comte, P. Vouaux, A new method of emission of light by certain organic compounds, J. Chim. Phys. 50 (1953) 64.

[2] M. Pope, H. Kallmann, P. Magnante, Electroluminescence in organic crystals, J. Chem. Phys. 38 (1963) 2042-2043.

[3] M. Sano, M. Pope, H. Kallmann, Electroluminescence and band gap in anthracene, J. Chem. Phys. 43 (1965) 2920-2921.

[4] P. Vincett, W. Barlow, R. Hann, G. Roberts, Electrical conduction and low voltage blue electroluminescence in vacuum-deposited organic films, Thin Solid Films. 94 (1982) 171-183.

[5] C.W. Tang, S.A. VanSlyke, Organic electroluminescent diodes, Appl. Phys. Lett. 51 (1987) 913-915.

[6] J. Burroughes, D. Bradley, A. Brown, R. Marks, K. Mackay, R. Friend, P. Burns, A. Holmes, Light-emitting diodes based on conjugated polymers, Nature. 347 (1990) 539-541.

[7] M. Baldo, D. O'brien, Y. You, A. Shoustikov, S. Sibley, M. Thompson, S. Forrest, Highly efficient phosphorescent emission from organic electroluminescent devices, Nature. 395 (1998) 151-154.

[8] C. Adachi, M.A. Baldo, M.E. Thompson, S.R. Forrest, Nearly 100% internal phosphorescence efficiency in an organic light-emitting device, J. Appl. Phys. 90 (2001) 5048-5051.

[9] S. Reineke, G. Schwartz, K. Walzer, M. Falke, K. Leo, Highly phosphorescent organic mixed films: The effect of aggregation on triplet-triplet annihilation, Appl. Phys. Lett. 94 (2009) 163305-163305-3.

[10] M.A. Baldo, S. Lamansky, P.E. Burrows, M.E. Thompson, S.R. Forrest, Very high-efficiency green organic light-emitting devices based on electrophosphorescence, Appl. Phys. Lett. 75 (1999) 4-6.

[11] S. Liu, B. Li, L. Zhang, H. Song, H. Jiang, Enhanced efficiency and reduced roll-off in nondoped phosphorescent organic light-emitting devices with triplet multiple quantum well structures, Appl. Phys. Lett. 97 (2010) 083304-083304-3.

[12] G. Lei, L. Wang, Y. Qiu, Improved Performance of Electrophosphorescent Organic Light-emitting Diode by Graded Doped Emissive Layer, Jpn. J. Appl. Phys. 43 L1226.

[13] Z. . Gao, B. . Mi, H. . Tam, K. . Cheah, C. . Chen, M. . Wong, S. . Lee, C. . Lee, High Efficiency and Small Roll-Off Electrophosphorescence from a New Iridium Complex with Well-Matched Energy Levels, Adv Mater. 20 (2008) 774-778.

[14] H. Lee, S.W. Cho, K. Han, P.E. Jeon, C. Whang, K. Jeong, K. Cho, Y. Yi, The origin of the hole injection improvements at indium tin oxide/molybdenum trioxide/N,N[sup [prime]]-bis(1-naphthyl)-N,N[sup [prime]]-diphenyl-1,1[sup [prime]]-biphenyl- 4,4[sup [prime]]-diamine interfaces, Appl. Phys. Lett. 93 (2008) 043308-3.

[15] A.J. Makinen, I.G. Hill, Z.H. Kafafi, Vacuum level alignment in organic guest-host systems, J. Appl. Phys. 92 (2002) 1598-1603.

[16] W. Hung, Z. Chen, H. You, F. Fan, H. Chen, K. Wong, Efficient carrier- and exciton-confining device structure that enhances blue PhOLED efficiency and reduces efficiency roll-off, Organic Electronics: physics, materials, applications. 12 (2011) 575-581.

[17] G. Gu, D.Z. Garbuzov, P.E. Burrows, S. Venkatesh, S.R. Forrest, M.E. Thompson, High-external-quantum-efficiency organic light-emitting devices, Opt. Lett. 22 (1997) 396-398.

[18] C.C. Wu, C.I. Wu, J.C. Sturm, A. Kahn, Surface modification of indium tin oxide by plasma treatment: An effective method to improve the efficiency, brightness, and reliability of organic light emitting devices, Appl. Phys. Lett. 70 (1997) 1348-1350.

[19] Z.D. Popovic, H. Aziz, Reliability and degradation of small molecule-based organic light-emitting devices (OLEDs), IEEE Journal on Selected Topics in Quantum Electronics. 8 (2002) 362-371.

[20] H. Aziz, Z.D. Popovic, N. Hu, A. Hor, G. Xu, Degradation mechanism of small molecule-based organic light-emitting devices, Science. 283 (1999) 1900-1902.

[21] M.A. Baldo, D.F. O'Brien, Y. You, A. Shoustikov, S. Sibley, M.E. Thompson, S.R. Forrest, Highly efficient phosphorescent emission from organic electroluminescent devices, Nature. 395 (1998) 151-154.

[22] N. Chopra, J. Lee, Y. Zheng, S. Eom, J. Xue, F. So, High efficiency blue phosphorescent organic light-emitting device, Appl. Phys. Lett. 93 (2008) 143307-3.

[23] N.C. Giebink, B.W. DAndrade, M.S. Weaver, P.B. Mackenzie, J.J. Brown, M.E. Thompson, S.R. Forrest, Intrinsic luminance loss in phosphorescent small-molecule organic light emitting devices due to bimolecular annihilation reactions, J. Appl. Phys. 103 (2008) 044509-1.

[24] Z.D. Popovic, H. Aziz, Delayed electroluminescence: a new tool for studies of OLED fundamental properties, Proceedings of the SPIE - The International Society for Optical Engineering. 5937 (2005) 59370-1.

[25] C. Adachi, M.A. Baldo, M.E. Thompson, S.R. Forrest, Nearly 100% internal phosphorescence efficiency in an organic light-emitting device, J. Appl. Phys. 90 (2001) 5048-5051.

[26] B. . - D'Andrade, S. . - Forrest, - White Organic Light-Emitting Devices for Solid-State Lighting, - Advanced Materials. - 1585.

[27] Liisa Halonen, Eino Tetri and Pramod Bhusal, Guidebook on Energy Efficient Electric Lighting for Buildings (Annex 45 - Energy Efficient Electric Lighting for Buildings) , (2010).

[28] S. Reineke, F. Lindner, G. Schwartz, N. Seidler, K. Walzer, B. Lussem, K. Leo, White organic light-emitting diodes with fluorescent tube efficiency, Nature. 459 (2009) 234-238.

[29] M.A. Baldo, C. Adachi, S.R. Forrest, Transient analysis of organic electrophosphorescence. II.â€ƒTransient analysis of triplet-triplet annihilation, Phys. Rev. B. 62 (2000) 10967-10977.

[30] M. Cocchi, V. Fattori, D. Virgili, C. Sabatini, P. Di Marco, M. Maestri, J. Kalinowski, Highly efficient organic electrophosphorescent light-emitting diodes with a reduced quantum efficiency roll off at large current densities, Appl. Phys. Lett. 84 (2004) 1052-1054.

[31] M. Lee, J. Lin, M. Chu, M. Tseng, Suppression of efficiency roll off in blue phosphorescent organic light-emitting devices using double emission layers with additional carrier-transporting material, Appl. Phys. Lett. 94 (2009) 083506.

[32] S. Reineke, K. Walzer, K. Leo, Triplet-exciton quenching in organic phosphorescent light-emitting diodes with Ir-based emitters, Phys. Rev. B. 75 (2007) 125328.

[33] D. Song, S. Zhao, Y. Luo, H. Aziz, Causes of efficiency roll-off in phosphorescent organic light emitting devices: Triplet-triplet annihilation versus triplet-polaron quenching, Appl. Phys. Lett. 97 (2010) 243304.

[34] S. Reineke, G. Schwartz, K. Walzer, K. Leo, Direct observation of hostâ€“guest tripletâ€“triplet annihilation in phosphorescent solid mixed films, phys. stat. sol. (RRL). 3 (2009) 67-69.

[35] A. Laaperi, OLED lifetime issues from a mobile-phone-industry point of view, Journal of the Society for Information Display. 16 (2008) 1125-1130.

[36] H. Aziz, Z. Popovic, S. Xie, A. Hor, N. Hu, C. Tripp, G. Xu, Humidity-induced crystallization of tris (8-hydroxyquinoline) aluminum layers in organic light-emitting devices, Appl. Phys. Lett. 72 (1998) 756-758.

[37] J. McElvain, H. Antoniadis, M.R. Hueschen, J.N. Miller, D.M. Roitman, J.R. Sheats, R.L. Moon, Formation and growth of black spots in organic light-emitting diodes, J. Appl. Phys. 80 (1996) 6002-7.

[38] S.Y. Kim, K.Y. Kim, Y. Tak, J. Lee, Dark spot formation mechanism in organic light emitting diodes, Appl. Phys. Lett. 89 (2006).

[39] P.E. Burrows, V. Bulovic, S.R. Forrest, L.S. Sapochak, D.M. McCarty, M.E. Thompson, Reliability and degradation of organic light emitting devices, Appl. Phys. Lett. 65 (1994) 2922-2924.

[40] S. Scholz, R. Meerheim, K. Walzer, K. Leo, Chemical degradation mechanisms of organic semiconductor devices, 6999 (2008) SPIE Europe; Alsace International; Conseil General du Bas-Rhin; Region Alsace; Communaute Urbaine de Strasbourg.

[41] N.C. Giebink, B.W. D'Andrade, M.S. Weaver, J.J. Brown, S.R. Forrest, Direct evidence for degradation of polaron excited states in organic light emitting diodes, 105 (2009).

[42] H. Bässler, A. Köhler, Charge transport in organic semiconductors, in: Anonymous Unimolecular and Supramolecular Electronics I, Springer, 2012, pp. 1-65.

[43] V. Coropceanu, J. Cornil, da Silva Filho, Demetrio A, Y. Olivier, R. Silbey, J. Brédas, Charge transport in organic semiconductors, Chemical Reviews-Columbus. 107 (2007) 926-952.

[44] F. Ortmann, F. Bechstedt, K. Hannewald, Theory of charge transport in organic crystals: Beyond Holstein's small-polaron model, Physical Review B. 79 (2009) 235206.

[45] H. Bässler, Charge transport in disordered organic photoconductors a Monte Carlo simulation study, physica status solidi (b). 175 (1993) 15-56.

[46] D. Hertel, H. Bässler, U. Scherf, H. Hörhold, Charge carrier transport in conjugated polymers, J. Chem. Phys. 110 (1999) 9214.

[47] A. Monkman, Singlet Generation from Triplet Excitons in Fluorescent Organic Light-Emitting Diodes, ISRN Materials Science. 2013 (2013).

[48] R. Kepler, J. Caris, P. Avakian, E. Abramson, Triplet excitons and delayed fluorescence in anthracene crystals, Phys. Rev. Lett. 10 (1963) 400-402.

[49] H. Sternlicht, G. Nieman, G. Robinson, Triplet—Triplet Annihilation and Delayed Fluorescence in Molecular Aggregates, J. Chem. Phys. 38 (1963) 1326.

[50] D. Hertel, H. Bässler, R. Guentner, U. Scherf, Triplet-triplet annihilation in a poly (fluorene)-derivative, J. Chem. Phys. 115 (2001) 10007.

[51] J. Partee, E. Frankevich, B. Uhlhorn, J. Shinar, Y. Ding, T. Barton, Delayed fluorescence and triplet-triplet annihilation in π-conjugated polymers, Phys. Rev. Lett. 82 (1999) 3673-3676.

[52] D.Y. Kondakov, Role of triplet-triplet annihilation in highly efficient fluorescent devices, Journal of The Society for Information Display. 17 (2009) 137-144.

[53] D. Kondakov, T. Pawlik, T. Hatwar, J. Spindler, Triplet annihilation exceeding spin statistical limit in highly efficient fluorescent organic light-emitting diodes, J. Appl. Phys. 106 (2009) 124510-124510-7.

[54] B.H. Wallikewitz, D. Kabra, S. Gélinas, R.H. Friend, Triplet dynamics in fluorescent polymer light-emitting diodes, Physical Review B. 85 (2012) 045209.

[55] D. Hertel, K. Meerholz, Triplet-polaron quenching in conjugated polymers, The Journal of Physical Chemistry B. 111 (2007) 12075-12080.

[56] J. Lee, J. Lee, K. Song, S.J. Lee, H.Y. Chu, Influence of doping profile on the efficiency of blue phosphorescent organic light-emitting diodes, Appl. Phys. Lett. 92 (2008) 133304-133304-3.

[57] J. Lee, J. Lee, J. Lee, H.Y. Chu, Effects of charge balance on device performances in deep blue phosphorescent organic light-emitting diodes, Organic Electronics. 11 (2010) 1159-1164.

[58] F. Zang, T. Sum, A. Huan, T. Li, W. Li, F. Zhu, Reduced efficiency roll-off in phosphorescent organic light emitting diodes at ultrahigh current densities by suppression of triplet-polaron quenching, Appl. Phys. Lett. 93 (2008) 023309-023309-3.

[59] B. Diouf, W.S. Jeon, R. Pode, J.H. Kwon, Efficiency Control in Iridium Complex-Based Phosphorescent Light-Emitting Diodes, Advances in Materials Science and Engineering. 2012 (2012).

[60] Z.B. Wang, M.G. Helander, Z.W. Liu, M.T. Greiner, J. Qiu, Z.H. Lu, Controlling carrier accumulation and exciton formation in organic light emitting diodes, Appl. Phys. Lett. 96 (2010) 043303-3.

[61] M. Baldo, S. Forrest, Transient analysis of organic electrophosphorescence: I. Transient analysis of triplet energy transfer, Physical Review B. 62 (2000) 10958.

[62] E.L. Williams, K. Haavisto, J. Li, G.E. Jabbour, Excimer-based white phosphorescent organic light-emitting diodes with nearly 100% internal quantum efficiency, Adv Mater. 19 (2007) 197-202.

[63] K.S. Yook, J.Y. Lee, Recombination zone study of phosphorescent organic light-emitting diodes with triplet mixed host emitting structure, Journal of Industrial and Engineering Chemistry. 16 (2010) 181-184.

[64] F. So, D. Kondakov, Degradation mechanisms in small-molecule and polymer organic light-emitting diodes, Adv Mater. 22 (2010) 3762-3777.

[65] Z.D. Popovic, S. Xie, N. Hu, A. Hor, D. Fork, G. Anderson, C. Tripp, Life extension of organic LED's by doping of a hole transport layer, Thin Solid Films. 363 (2000) 6-8.

[66] Y. Luo, H. Aziz, G. Xu, Z.D. Popovic, Electron-induced quenching of excitons in luminescent materials, Chemistry of Materials. 19 (2007) 2288-91.

[67] D.Y. Kondakov, W.C. Lenhart, W.F. Nichols, Operational degradation of organic light-emitting diodes: mechanism and identification of chemical products, J. Appl. Phys. 101 (2007) 24512-1.

[68] S.T. Lee, Z.Q. Gao, L.S. Hung, Metal diffusion from electrodes in organic light-emitting diodes, Appl. Phys. Lett. 75 (1999) 1404-1406.

[69] V. Sivasubramaniam, F. Brodkorb, S. Hanning, O. Buttler, H.P. Loebl, V. van Elsbergen, H. Boerner, U. Scherf, M. Kreyenschmidt, Degradation of HTL layers during device operation in PhOLEDs, Solid State Sciences. 11 (2009) 1933-1940.

[70] N. Giebink, S. Forrest, Quantum efficiency roll-off at high brightness in fluorescent and phosphorescent organic light emitting diodes, Physical Review B. 77 (2008) 235215.

[71] R. Meerheim, S. Scholz, S. Olthof, G. Schwartz, S. Reineke, K. Walzer, K. Leo, Influence of charge balance and exciton distribution on efficiency and lifetime of phosphorescent organic light-emitting devices, J. Appl. Phys. 104 (2008).

[72] K. Goushi, R. Kwong, J.J. Brown, H. Sasabe, C. Adachi, Triplet exciton confinement and unconfinement by adjacent hole-transport layers, J. Appl. Phys. 95 (2004) 7798-7802.

[73] M. Pfeiffer, S.R. Forrest, K. Leo, M.E. Thompson, Electrophosphorescent pin organic light-emitting devices for very-high-efficiency flat-panel displays, Adv Mater. 14 (2002) 1633-1636.

[74] S.Y. Kim, W.S. Jeon, T.J. Park, R. Pode, J. Jang, J.H. Kwon, Low voltage efficient simple< equation> pin</equation> type electrophosphorescent green organic light-emitting devices, Appl. Phys. Lett. 94 (2009) 133303-133303-3.

[75] B.W. DAndrade, M.A. Baldo, C. Adachi, J. Brooks, M.E. Thompson, S.R. Forrest, High-efficiency yellow double-doped organic light-emitting devices based on phosphor-sensitized fluorescence, Appl. Phys. Lett. 79 (2001) 1045-1047.

[76] B.D. Chin, M.C. Suh, M. Kim, S.T. Lee, H.D. Kim, H.K. Chung, Carrier trapping and efficient recombination of electrophosphorescent device with stepwise doping profile, Appl. Phys. Lett. 86 (2005) 133505-133505-3.

[77] W.S. Jeon, T.J. Park, S.Y. Kim, R. Pode, J. Jang, J.H. Kwon, Ideal host and guest system in phosphorescent OLEDs, Organic Electronics. 10 (2009) 240-246.

[78] D. Song, S. Zhao, Y. Luo, H. Aziz, Causes of efficiency roll-off in phosphorescent organic light emitting devices: Triplet-triplet annihilation versus triplet-polaron quenching, Appl. Phys. Lett. 97 (2010) 243304-3.

[79] Y. Chang, D.P. Puzzo, Z. Wang, M.G. Helander, J. Qiu, J. Castrucci, Z. Lu, Improving the efficiency of red phosphorescent organic light emitting diodes by exciton management, physica status solidi (c). 9 (2012) 2537-2540.

[80] J.H. Kwon, W.S. Jeon, T.J. Park, 23.4: Invited Paper: Ideal Host-Dopant System for Highly Efficient Phosphorescent OLEDs, 40 (2009) 317-320.

[81] Z.B. Wang, M.G. Helander, J. Qiu, D.P. Puzzo, M.T. Greiner, Z.W. Liu, Z.H. Lu, Highly simplified phosphorescent organic light emitting diode with > 20% external quantum efficiency at > 10,000 cd/m[sup 2], Appl. Phys. Lett. 98 (2011) 073310-3.

[82] Y. Kawamura, K. Goushi, J. Brooks, J.J. Brown, H. Sasabe, C. Adachi, 100% phosphorescence quantum efficiency of Ir (III) complexes in organic semiconductor films, Appl. Phys. Lett. 86 (2005) 071104.

[83] Y. Tao, Q. Wang, C. Yang, Q. Wang, Z. Zhang, T. Zou, J. Qin, D. Ma, A simple carbazole/oxadiazole hybrid molecule: an excellent bipolar host for green and red phosphorescent OLEDs, Angewandte Chemie. 120 (2008) 8224-8227.

[84] Y.Q. Zhang, G.Y. Zhong, X.A. Cao, Concentration quenching of electroluminescence in neat Ir(ppy)sub 3] organic light-emitting diodes, J. Appl. Phys. 108 (2010) 083107-5.

[85] V.I. Adamovich, S.R. Cordero, P.I. Djurovich, A. Tamayo, M.E. Thompson, B.W. D'Andrade, S.R. Forrest, New charge-carrier blocking materials for high efficiency OLEDs, Organic electronics. 4 (2003) 77-87.

[86] K. Goushi, R. Kwong, J.J. Brown, H. Sasabe, C. Adachi, Triplet exciton confinement and unconfinement by adjacent hole-transport layers, J. Appl. Phys. 95 (2004) 7798-7802.

[87] G.J. McGraw, D.L. Peters, S.R. Forrest, Organic vapor jet printing at micrometer resolution using microfluidic nozzle arrays, Appl. Phys. Lett. 98 (2011) 013302.

[88] H. Zamani Siboni, H. Aziz, The influence of the hole blocking layers on the electroluminescence stability of phosphorescent organic light emitting devices, Organic Electronics. 12 (2011) 2056-2060.

[89] Y. Luo, H. Aziz, Probing triplet-triplet annihilation zone and determining triplet exciton diffusion length by using delayed electroluminescence, J. Appl. Phys. 107 (2010) 094510.

[90] D. Song, Q. Wang, S. Zhao, H. Aziz, Dependence of carrier recombination mechanism on the thickness of the emission layer in green phosphorescent organic light emitting devices, Organic Electronics. 12 (2011) 582-588.

[91] H.Z. Siboni, Y. Luo, H. Aziz, Luminescence degradation in phosphorescent organic light-emitting devices by hole space charges, J. Appl. Phys. 109 (2011) 044501-6.

[92] J.Y. Lee, Effect of doping profile on the lifetime of green phosphorescent organic light-emitting diodes, Appl. Phys. Lett. 89 (2006) 153503.

[93] B.D. Chin, C. Lee, Confinement of charge carriers and excitons in electrophosphorescent devices: Mechanism of light emission and degradation, Adv Mater. 19 (2007) 2061-2066.

[94] Y. Tsai, S. Wang, S. Chen, S. Su, F. Juang, Efficiency improvement of flexible fluorescent and phosphorescent organic light emitting diodes by inserting a spin-coating buffer layer, Thin Solid Films. 517 (2009) 5338-5342.

[95] J. Kang, D. Lee, H. Park, J.W. Kim, W. Jeong, Y. Park, S. Lee, K. Go, J. Lee, J. Kim, A host material containing tetraphenylsilane for phosphorescent OLEDs with high efficiency and operational stability, Organic Electronics. 9 (2008) 452-460.

[96] R.C. Kwong, M.R. Nugent, L. Michalski, T. Ngo, K. Rajan, Y. Tung, M.S. Weaver, T.X. Zhou, M. Hack, M.E. Thompson, S.R. Forrest, J.J. Brown, High operational stability of electrophosphorescent devices, Appl. Phys. Lett. 81 (2002) 162-164.

[97] K.M. Vaeth, C.W. Tang, Light-emitting diodes based on phosphorescent guest/polymeric host systems, J. Appl. Phys. 92 (2002) 3447-53.

[98] Young Wook Park, Young Min Kim, Jin Hwan Choi, Tae Hyun Park, Jin-Wook Jeong, Hyun Ju Choi, Byeong Kwon Ju, Enhanced Electroluminescence Efficiency of Phosphorescent

Organic Light-Emitting Diodes by Controlling the Triplet Energy of the Hole-Blocking Layer, Electron Device Letters, IEEE. 31 (2010) 452-454.

[99] D.C. Byung, C.S. Min, Mu-Hyun Kim, T.L. Seong, D.K. Hye, K.C. Ho, Carrier trapping and efficient recombination of electrophosphorescent device with stepwise doping profile, Appl. Phys. Lett. 86 (2005) 133505-1.

[100] Z.D. Popovic, H. Aziz, Delayed electroluminescence in small-molecule-based organic light-emitting diodes: Evidence for triplet-triplet annihilation and recombination-center-mediated light-generation mechanism, J. Appl. Phys. 98 (2005) 013510-013510-5.

[101] E. Tutis, D. Berner, L. Zuppiroli, Internal electric field and charge distribution in multilayer organic light-emitting diodes, J. Appl. Phys. 93 (2003) 4594-602.

[102] D.Y. Kondakov, J.R. Sandifer, C.W. Tang, R.H. Young, Nonradiative recombination centers and electrical aging of organic light-emitting diodes: Direct connection between accumulation of trapped charge and luminance loss, J. Appl. Phys. 93 (2003) 1108-1119.

[103] Y. Luo, H. Aziz, Space charge effects on the electroluminescence efficiency and stability of organic light-emitting devices with mixed emitting layers, Appl. Phys. Lett. 95 (2009) 073304.

[104] J. Lee, J. Lee, J. Lee, H.Y. Chu, Effects of charge balance on device performances in deep blue phosphorescent organic light-emitting diodes, Organic Electronics: physics, materials, applications. 11 (2010) 1159-1164.

[105] D.Y. Kondakov, W.F. Nichols, W.C. Lenhart, Distinguished paper: Structural identification of chemical products and mechanism of operational degradation of OLEDs, 38 (2007) 1494-1496.

[106] S.T. Lee, Z.Q. Gao, L.S. Hung, Metal diffusion from electrodes in organic light-emitting diodes, Appl. Phys. Lett. 75 (1999) 1404-1406.

[107] J. Kang, S. Lee, H. Park, W. Jeong, K. Yoo, Y. Park, J. Kim, Low roll-off of efficiency at high current density in phosphorescent organic light emitting diodes, Appl. Phys. Lett. 90 (2007) 223508.

[108] N. Matsusue, S. Ikame, Y. Suzuki, H. Naito, Charge carrier transport in an emissive layer of green electrophosphorescent devices, Appl. Phys. Lett. 85 (2004) 4046-4048.